Stony Brook University

Analysis of short range entangled topological phases protected by time-reversal symmetry

A Thesis presented

by

Sebastian Dick

to

The Graduate School

in Partial Fulfillment of the

Requirements

for the Degree of

Master of Arts

in

Physics

Stony Brook University

August 2015

Stony Brook University

The Graduate School

Sebastian Dick

We, the thesis committe for the above candidate for the

Master of Arts degree, hereby recommend

acceptance of this thesis

Dr. Lukasz Fidkowski - Thesis Advisor
Assistant Professor, Department of Physics and Astronomy

Dr. Tzu-Chieh Wei - Second Reader
Assistant Professor, C.N. Yang Institute for Theoretical Physics

Dr. Dominik Schneble
Associate Professor, Department of Physics and Astronomy

This thesis is accepted by the Graduate School

Charles Taber
Dean of the Graduate School

Abstract of the Thesis

Analysis of short range entangled topological phases protected by time-reversal symmetry

by

Sebastian Dick

Master of Arts

in

Physics

Stony Brook University

2015

We discuss a short-range entangled topological phase in 3+1 dimensions that is protected by time-reversal symmetry. Two models are compared that realize this phase: The first is a construction developed by Chen, Gu, Liu and Wen, which encodes the system's topological properties in the representation of the symmetry group. The second theory uses a non-linear sigma model in which the distinct topological phases differ by the way the symmetry acts on the order parameter. Both theories have in common that the modeled phases are in one to one correspondence with the elements of the cohomology group $\mathcal{H}^{d+1}(\mathbb{Z}_2^T, U_T(1))$. In this work, we extend the Chen-Gu construction to 3+1 dimensional systems. Furthermore, we show that both models coincide with respect to their topological properties. This is proved by comparing spin-flip processes and their associated topological phase factors. We derive spin-flip operators on the surface of the (3+1)-dimensional Chen-Gu construction that commute with time-reversal symmetry. To implement spin-flip processes in the non-linear sigma model, we interpolate spin-configurations from a discrete, triangular lattice into the continuum. We proceed by analyzing the phases, generated by the θ-term, for spacetime configurations of the O(4) order parameter that correpond to these spin-flip processes.

Contents

1 Introduction **1**
1.1 Topology in condensed matter physics 1
1.2 Outline 3

2 Chen-Gu construction **5**
2.1 Classification of phases by entanglement 5
2.2 Tensor networks and local unitary transformations 6
2.3 Projective representations 7
2.4 Construction of SPT-wavefunctions 9
2.5 Summary 14

3 Non-linear sigma model **15**
3.1 Classification of SPT phases 15
3.2 θ-term and the Heisenberg chain 16
3.3 Boundaries and the WZW-term 18

4 Connection between NLSM and Chen-Gu construction **23**
4.1 Outline 23
4.2 Chen-Gu construction on a triangular lattice 23
4.3 Spin flip operators in the NLSM 27
4.4 Commutation relations for neighboring spin flips 29
4.5 Square of the spin flip 32

5 Conclusion and Outlook **34**

A Group cohomology **38**

B Alternative approach to connecting both theories **41**

C Tables **42**

List of Figures

1 a) Areas for coupling constant. b) Classification of topological phases . . 3
2 a) Canonical form for a 2+1 dimensional SRE state. b) Entanglement structure of 1D SPT 6
3 a) Labeling of partons. b) Cancellation of triangles 12
4 Transition to triangular lattice 13
5 Skyrmion configuration 17
6 a) Domain wall. b) Extension of spin-configuration 20
7 a) Areas for spin configuration. b) Evaluation of $\chi(r)$. c) Spin-down bonds 24
8 a) Site labeling. b) $\gamma = -1$ configurations. c) Spactime prism 26
9 Interpolation rules 28
10 Symmetry properties of prisms 29
11 Commutation relation for neighboring spin-flips 30
12 Square of the spin-flip 32
13 a) Branching structure on a 2 dimensional simplex. b) 3 dimensional simplex. 40

List of Tables

1 Surface configurations that bind a vortex 42
2 Geometrical phase associated with configurations on a prism 43
3 Derivation of the phase factor β 44

Acknowledgements

I would like to express deep thanks to my advisor Dr. Lukasz Fidkowski, who not only provided useful guidance whenever I was facing problems in my research, but also taught me a lot about the broad field of theoretical condensed matter physics, in his lecture, but also during private conversations.

I am very grateful for all the inspiring discussion that I had with Hendrik Poulsen Nautrup, and for his critical evaluation of parts of my work.

I would also like to thank Dr. Tzu-Chieh Wei and Dr. Dominik Schneble for being members of the defense committee.

Moreover, my thanks go to the Stony Brook University and the Julius-Maximilians-Universät Würzburg for making all this possible through their long-lasting exchange-program. In particular, I would like to thank Dr. Jacobus Verbaarschot and Sarah Lutterbie for being such a great help throughout the year.

I am deeply indebted to my family and my partner for their unconditional support.

1 Introduction

1.1 Topology in condensed matter physics

It has long been held that Landau symmetry breaking theory provides a complete description and classification of all phases of matter. Landau's theory states that the free energy of a system is analytic and can be written as a Taylor-expansion in the order-parameter around the critical temperature [14]. Therefore, within the Landau framework, all disordered systems, for which the order parameter vanishes, belong to the same trivial class.

However, recent findings, most notably the discovery of fractional quantum hall (FQH) systems, marked the beginning of a new era in condensed matter physics. The FQH effect suggests that even in classically disordered systems, where the correlation length is equal to the lattice spacing and there is no symmetry breaking, there can still be some kind of order, namely topological order [18].

Systems that exhibit this intrinsic topological order, some of which are the so-called topological spin-liquids, show a variety of interesting properties. Firstly, their ground state degeneracy depends on the topology of the manifold on which they are defined. Furthermore, topological phases of matter show fractional excitations, which carry only fractions of elementary quantum numbers (such as the electrical charge.) This is impressively shown in FQH, where the Laughlin quasiparticles carry charge $Q = \nu e$ (ν^{-1} is an odd number) [15]. Also these fractional excitations can obey anyonic statistics. Anyons only exist in two spatial dimensions and can come in two different 'flavors.' They can be either abelian or non-abelian. The exchange of two non-distinguishable abelian anyons can lead to an arbitrary phase factor $e^{i\theta}$. This can be considered as an extension to Fermi-Dirac and Bose-Einstein statistics. The behavior of non-abelian anyons is even more unusual, as an exchange of particles can lead to a transformation of the whole state. Kitaev showed that modular tensor category theory provides a powerful framework to deal with said kind of excitations [12]. Moreover, entanglement entropy studies suggest that these phases can be characterized by their entanglement structure [13](see Ch. 2.1).

Another milestone in condensed matter physics was the discovery of topological insulators (TI) [10]. These materials are trivial when defined on a compact spacetime manifold, meaning that their bulk is gapped and does not allow for fractional excitations. If there is a symmetry present, however, their boundary is either gapless or spontaneously breaks this symmetry. These kind of phases are usually dubbed symmetry-protected topological (SPT) phases. Their remarkable features have led to great interest among scientists and what is believed to be a complete classification of free fermion SPT phases has been obtained [17]. Nevertheless, there are still many unresolved problems that arise when interactions are included. In their paper, Fidkowski and Kitaev have been able to show that the $\mathbb{Z}$-labeling of time-reversal invariant Majorana chains breaks down to $\mathbb{Z}_8$

if interactions are included [8, 19]. Unfortunately, thus far, there has been no general classification for interacting fermionic SPT phases in two or more dimensions.

Other studies have concentrated on bosonic SPT phases. In contrast to its fermionic counterpart, 'strong' interactions are required to ensure that the bulk is gapped and are therefore needed to realize an SPT phase [20]. Even though these systems are physically much harder to engineer due to the need for strong interactions, they are conceptually easier to handle. There is hope that, by gaining knowledge about strongly interacting bosonic systems, we will be able to draw conclusions regarding the behavior of fermionic interacting topological systems. The requirements for a bosonic SPT phase protected by the symmetry group G can be summarized as follows [3]:

1. If the system is defined on a (d+1)-dimensional compact spacetime manifold, it is fully gapped and non-degenerate.

2. In a system with a (d-1+1)-dimensional boundary where the symmetry G is preserved, the boundary is either gapless or degenerate.

3. It follows that the action of the symmetry on the boundary states is implemented in a way that is forbidden in purely (d-1+1)-dimensional systems.

A prominent example for bosonic SPT phases is given by the one-dimensional spin-1 Haldane chain, which is protected by spin-rotation and other symmetries [1, 4]. Its bulk is made up of spins that form valence bonds and it is gapped. Its edges, however, are occupied by a 'dangling' $\frac{1}{2}$-spin each. These edge spins transform under a projective representation of the protecting symmetry and form Kramer's pairs, leading to a ground-state degeneracy of two. The spin-1 Haldane or AKLT chain belongs to a more general class of so-called topological paramagnets, which are quantum magnets made up of strongly interacting quantum spins on a lattice. All members of these classes realize SPT phases insofar as their bulk is gapped and they have protected surface states [20].

A basic question is, how does the choice of a symmetry group G determine the number of distinct bosonic SPT phases? Only recently, Chen et al. have proposed a classification of bosonic SPT phases in arbitrary dimensions in terms of group cohomology [6]. Evidence suggests that this classification indeed captures most of the theoretically possible SPT phases. However, there are examples where the group cohomology approach fails to give a complete description. For instance $H^4(\mathbb{Z}_2^T, U_T(1)) = \mathbb{Z}_2$ suggests that there is only one non-trivial topological phase protected by time-reversal (T-reversal) symmetry in 3+1 dimensions. However, Chen, Burnell, Vishwanath and Fidkowski showed through making use of a Walker-Wang construction, that there is a possible phase beyond the group cohomology. This phase can realize a very particular state, namely the three-fermion $\mathbb{Z}_2$ topological order, on its surface [21, 5].

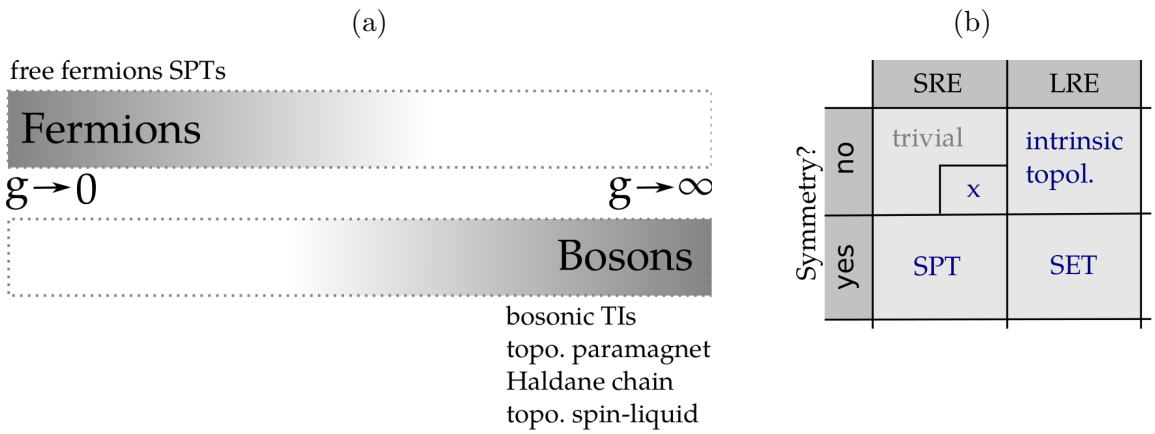

Figure 1: a) Areas for the coupling constant g for which a complete classification of topological phases exists. Examples for systems with topological order are given. b) Classification of topological phases according to their entanglement structure. The area labeled by x corresponds to phases that are SRE entangled but are topologically non-trivial even if there is no symmetry present.

In addition to SPT phases, there are topologically ordered systems in (2+1)-dimensions independent of symmetry that are trivial and gapped in the bulk but whose thermal Hall conductivity is quantized [12]. Also, starting with a LRE system, one can include symmetries, which leads to a broad variety of so-called symmetry-enriched topological (SET) phases. The field of SET phases is comparably young but significant progress has been made among others by an approach that, after gauging the protecting symmetry, attaches fractional symmetry quantum numbers to anyons, respecting the underlying fusion and braiding rules given by modular tensor category theory [7].

1.2 Outline

The aim of this work is to cast light on the different approaches used to classify and construct (3+1)-dimensional T-reversal invariant SPT phases. In particular, a precise connection between the cohomology construction made by Chen, Gu, Liu and Wen [6] and the non-linear sigma model (NLSM) description of SPT phases developed by Bi, Rasmussen, Slagle and Xu [3] is aimed at.

This thesis is structured as follows: In Ch. 2 we review the construction of SPT phases developed by Chen et al., and extend their construction to (3+1) dimensional systems with time(T)-reversal symmetry. The model they construct is based on the notion that SPT phases can be labeled by elements of the cohomology group $\mathcal{H}^{d+1}(G, U_T(1))$. The distinct phases differ by the way the symmetry G acts on them. The on-site representation of a group element g, $U^i(g)$ thereby includes cocycles $\nu(g_0, ..., g_n)$ that depend on the states which $U^i(g)$ acts on.

Ch. 3 deals with the description of SPT phases with NLSMs. We start by introducing the so-called θ-term, a topological term that measures the winding number of a mapping

$S^n \to S^n$. We further proceed by proving that the boundary of a system that is described by a NLSM with θ-term is described by a NLSM with WZW-term at level 1. As an example we derive the edge states of a 1+1d spin-1 Heisenberg chain. Finally we show that, by integrating out one component of the order parameter, the WZW-term of the boundary theory can be reduced to a θ-term, a result that is very important for the computations in the last section of this thesis.

Eventually, in Ch. 4 we try to connect both models mentioned above. This is done by defining spin-flip operators in both systems and comparing their respective properties. These properties are given by the commutation relations for neighboring spin flips and the eigenvalues of the squared spin flip operators.

2 Chen-Gu construction

2.1 Classification of phases by entanglement

Dealing with topology in condensed matter systems, one encounters a wide variety of different possible phases. Over the last decades, physicists have been looking for criteria to classify and distinguish between these phases. One of these criteria is believed to be provided by the entanglement structure of the ground state. Entanglement entropy studies strongly suggest that in systems where there is intrinsic topological order, meaning that there are fractional excitations and a ground state degeneracy, the different lattice sites are entangled over a long range. In long-range entangled systems the ground state cannot be continuously connected to a product state by local unitary (LU) transformations (see Sec. 2.2)[13]. It is believed that this long-range entanglement (LRE) provides a robust way to decide whether the system exhibits topological order or not.

If the system's entanglement structure is short ranged (i.e. if there is no LRE) there is no intrinsic topological order and the bulk is gapped and trivial [6, 20]. One might think that all gapped Hamiltonians that realize short-range entanglement (SRE) are trivial and belong to the same universality class, however, this is not entirely true. In fact, it turns out that if we include an on-site symmetry, the space of all SRE phases splits up into subspaces. As long as the symmetry is not broken, in taking a continuous path in Hamiltonian space from two distinct such components, one necessarily encounters a closing of the gap, implying a second-order phase transition. It is therefore in principle possible to classify Hamiltonians by the SRE phase that they realize. Non-trivial SRE phases protected by an on-site symmetry thereby correspond to the SPT phases mentioned above (Fig. 1b)

Chen et al. suggested in their paper that SPT phases protected by the on-site symmetry group G in d+1 spacetime dimensions are in one to one correspondence with a mathematical structure called the cohomology group $\mathcal{H}^{1+d}(G, U_T(1))$ (see App. A). The different group elements thereby correspond to distinct SPT-phases that cannot be connected without closing the gap [6]. It is important to note that this theory is merely at the level of a conjecture. Some phases that were theorized by Chen et al. have subsequently been shown to be non-trivial SPTs, however this is not the case for all of them. In particular there has been no definite proof that the T-reversal SPT treated in this thesis is in fact a non-trivial SPT phase. We follow the procedure described in Chen et al.'s paper to construct a 3+1 dimensional time reversal invariant SPT phase. We are going to refer to this model as the "Chen-Gu construction" throughout the thesis.

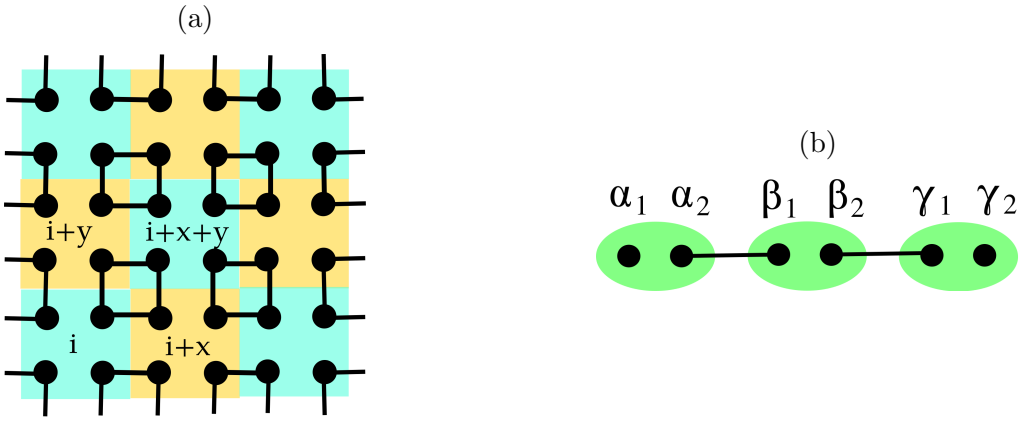

Figure 2: a) Canonical form for a 2+1 dimensional SRE state. The colors encode different effective sites whereas black dots corresponds to partons. Partons that share an edge are entangled. b) Entanglement structure of a 1-dimensional SPT state with open boundary conditions.

2.2 Tensor networks and local unitary transformations

In the following, we consider SRE states, i.e. states that can be transformed into a direct product state by local unitary (LU) transformations. To understand what a LU transformation is, let us introduce so-called piecewise LU operators, given by

$$U_{pwlu} = \prod_i U^i, \tag{1}$$

where U^i are unitary operators that act on non-overlapping regions in spacetime. We can use M piecewise LU operators to build a so-called quantum circuit with depth M:

$$U^M_{circ} = U^{(1)}_{pwlu} U^{(2)}_{pwlu} ... U^{(M)}_{pwlu} \tag{2}$$

This quantum circuit of finite depth (meaning it does not scale with the system size) is commonly referred to as a LU transformation.

To make general statements about SRE phases it would be desirable to have a canonical form for the entanglement structure. A convenient way to depict this structure is to make use of tensor network (TN) diagrams. In a TN diagram, every dot corresponds to a tensor and every edge attached to the dot corresponds to an index. An edge connecting two dots depicts a contraction of the two connected indices, therefore, sites (tensors) that are connected by an edge are entangled.

Let us now make use of the fact that an SRE state can always be transformed into a direct product state by LU transformations. Given an arbitrary entanglement structure, we can choose our effective sites sufficiently large for every effective site to be only entangled with its nearest neighbors.

The definition of SRE states makes sure that this "coarse-graining" procedure is

always possible. We can now use LU transformations to move the original sites, which we are going to refer to as partons, inside of the effective sites to obtain a structure shown in Fig. 2a. The structure obtained makes it very clear that the wavefunction can be written as a direct product state.

As mentioned above, without symmetry, all SRE states are the same, meaning that one can always go over from one state to another by acting with LU transformations. This implies that all SRE states belong to the same phase.

However, if we include an on-site symmetry G and impose that it cannot be broken, this adds a restriction to the allowed LU transformations, making sure that only LU transformations that respect the symmetry may be used. This however has the effect that not all SRE states can be connected to one another. The phase space therefore splits up into different distinct SPT phases.

2.3 Projective representations

This section will give an introduction to so-called projective representations. We will show that the projective representations of a group G can be described by the second cohomology group $\mathcal{H}^2(G, U_T(1))$. This result is particularly important for 1+1 dimensional SPT phases and was generalized by Chen et al. to arbitrary dimensions. A more general introduction to group cohomology can be found in Appendix A.

Let us consider a group G with elements $g_1, g_2 \in G$. A linear representation of G is given by matrices $U(g)$ if they obey

$$U(g_1)U(g_2) = U(g_1 g_2). \tag{3}$$

This definition can be extended to groups that contain time-reversal by

$$U(g_1)U_{s(g_1)}(g_2) = U(g_1 g_2) \tag{4}$$

where $U_{s(g_1)}(g_2) = (U(g_2))^*$ for $g_1 = T$ and $U_{s(g_1)}(g_2) = U(g_2)$ otherwise.

In quantum mechanics one is only interested in observable quantities and more often than not, wavefunctions are only defined up to an immeasurable phase factor. It is therefore only natural to introduce so called projective representations $V(g_1)$, that correspond to linear representations up to a phase factor $\omega(g_1, g_2) \in U(1)$,

$$V(g_1)V_{s(g_1)}(g_2) = \omega(g_1, g_2)V(g_1 g_2). \tag{5}$$

The phase factors are usually referred to as the factor system of the representation. Given that, in a physical system, it should not matter how subsequent operators are "grouped" before acting on the state, it makes sense to require that all representations

(even projective ones) obey associativity. This can be expressed as

$$\left[V(g_1)V_{s(g_1)}(g_2)\right] V_{s(g_1g_2)}(g_3) = V(g_1)\left[V(g_2)V_{s(g_2)}(g_3)\right]_{s(g_1)}, \tag{6}$$

which implies

$$\omega(g_1, g_2)\omega(g_1g_2, g_3) = \omega^{s(g_1)}(g_2, g_3)\omega(g_1, g_2g_3). \tag{7}$$

Now, distinct projective representations are characterized by their different factor systems. Note however, that we can re-define the matrices by a phase factor $V'(g) = \beta(g)V(g)$ resulting in a new factor system

$$\omega'(g_1, g_2) = \frac{\beta(g_1g_2)}{\beta(g_1)\beta^{s(g_1)}(g_2)}\omega(g_1, g_2). \tag{8}$$

Factor systems that are related by this relation are considered to describe the same projective representation. Note that Eq. 8 defines an equivalence relation. Therefore, the factor systems can be grouped into equivalence classes ω.

Furthermore, one can construct new representations by making use of the tensor product $V_1(g) \otimes V_2(g)$, which results in a new factor system $\omega_1(g)\omega_2(g)$. The associated class can be written as $\omega_1 + \omega_2$. It can be shown that the classes ω are elements of an Abelian group called the second cohomology group $\mathcal{H}^2(G, U_T(1))$. The $\omega(g_1, g_2)$ thereby correspond to so-called cocycles and the coboundaries are given by the term made up of $\beta(g)$. The cohomology group can therefore be written as a quotient group

$$\mathcal{H}^2(G, U_T(1)) = \frac{\text{Group of Cocycles}}{\text{Group of Coboundaries}}. \tag{9}$$

The trivial element of this group corresponds to the linear representation of G. A prominent example for a projective representation is the spin-1/2 representation of SO(3).

As an example, let us derive the different representations of the T-reversal group $\mathbb{Z}_2^T$. We can always write the representation of the T-reversal element as $M(T) = U(T)K$, where $U(T)$ is a unitary representation and K is the antiunitary operator that acts as complex conjugation, $Ka = a^*K$. The linear representation is simply given by the one dimensional representation $U(T) = e^{i\theta}$ where $\theta \in [0, 2\pi)$. Clearly, $M(T)M(T) = 1$ and $M(T)M(e) = U(T)K \cdot 1 = M(T)$, therefore $M(T)$ indeed forms a linear representation of $\mathbb{Z}_2^T$.

To find the projective representations we make use of the fact that $\mathcal{H}^2(\mathbb{Z}_2^T, U_T(1)) = \mathbb{Z}_2$ [6]. The T-reversal group has therefore one projective representation. We can freely choose (by a suitable gauge tranformation) $\omega(e, e) = 1$. This implies that $M(e)M(e) = M(e)$, and we can therefore set $M(e) = I$, where is I the identity matrix. Further

$M(T)M(T) = U(T)KU(T)K = \omega(T,T) = U(T)(U(T))^*$. This implies

$$U(T) = \omega(T,T)(U(T))^T = (\omega(T,T))^2 U(T) \quad \Rightarrow \quad \omega(T,T) = \pm 1. \tag{10}$$

It is straightforward to derive $\omega(e,T) = \omega(T,e) = \omega(e,e)$. We have therefore found the projective presentation given by $\omega(e,e) = \omega(e,T) = 1$ and $\omega(T,T) = -1$. An explicit construction for this representation is given by the 2-dimensional matrices

$$U(e) = \begin{pmatrix} 1 & 0 \\ 0 & 1 \end{pmatrix}; \quad U(T) = \begin{pmatrix} 0 & -1 \\ 1 & 0 \end{pmatrix} \tag{11}$$

In the following section we will see that the boundary states of a 1-dimensional SPT state transform projectively under the symmetry. This is impressively shown in an AKLT chain with open boundary conditions, which is known to realize SPT order. The dangling spin-$\frac{1}{2}$'s at each end of the chain transform as Kramer doublets under T-reversal, so that $M(T)M(T) = -1$. Chen et al. proposed that the general idea of projective representations of boundary states can be extended to d-dimensional systems by making use of the higher cohomology groups $\mathcal{H}^{d+1}(G, U_T(1))$.

2.4 Construction of SPT-wavefunctions

In their paper [6], Chen et al. suggest that wavefunctions belonging to distinct SPT phases differ in the way the on-site symmetry G acts on them. They all have in common that they are invariant under the global action of the symmetry transformation. If we denote the local symmetry transformation on site i by U^i, this means that

$$\otimes_i U^i \left|\psi\right\rangle = \left|\psi\right\rangle, \tag{12}$$

where $|\psi\rangle$ is a wavefunction describing the canonical state defined in section 2.2 and U^i has to form a linear representation of the symmetry group on each site. Different pairs (U^i, $|\psi\rangle$) can correspond to different SPT phases. This, however, is only true if they cannot be related by an equivalence relation. Let U^i and $\tilde{U}^i$ be two different representations of the same symmetry group G, then both representations characterize two different SPT phases only if $U^i \nsim \tilde{U}^i$. Two representations are said to be equivalent if

1. they are related by a unitary transformation W^i acting on the effective site:

$$\tilde{U}^i = W^i U^i W^{i\dagger}, \tag{13}$$

2. they differ by local degrees of freedom that form a 1d representation:

$$\tilde{U}^i = U^i \otimes V^{1,i} \otimes V^{2,i} \otimes V^{3,i} \otimes V^{4,i} \tag{14}$$
$$\text{given} \quad V^{1,i} \otimes V^{2,i+x} \otimes V^{3,i+x+y} \otimes V^{4,i+y} = 1 \oplus ...,$$

where $V^{a,i}_{\alpha,\beta}$ are linear representations of G (Fig. 2a).

The equivalence classes of symmetry transformations arising from the above definitions correspond to the different SPT-phases.

We now go over to explicitly constructing states that realize T-reversal invariant SPT phases in 3+1 dimensions. Let us review the construction for 1+1 dimensions given in the paper by Chen et al. We know that

$$\mathcal{H}^{n+1}(\mathbb{Z}_2^T, U_T(1)) = \mathbb{Z}_2$$

for n odd. Furthermore we know $\omega_4(g_0, g_1, g_2, g_3) = -1$ for $g_0, g_1, g_2, g_3 = T$ and $\omega_4(g_0, g_1, g_2, g_3) = 1$ otherwise [5]. Equivalently

$$\nu_4(1, T, 1, T, 1) = \nu_4(T, 1, T, 1, T) = -1 \tag{15}$$

and $\nu_4(g_0, g_1, g_2, g_3, g_4) = 1$ otherwise.

For their construction, Chen et al. choose the 1D wave function to be a "dimer crystal" (Fig. 2b) given by

$$|\psi\rangle = ... \otimes (\sum_{g\in G} |\alpha_2 = g, \beta_1 = g\rangle) \otimes (\sum_{g\in G} |\beta_2 = g, \gamma_1 = g\rangle) \otimes .... \tag{16}$$

Greek letters denote the different effective sites and the indices they carry denote the respective partons. It is clear that neighboring partons that belong to different sites form a maximally entangled state. The local symmetry transformation can now be chosen to act as

$$U^i(g)\,|\alpha_1, \alpha_2\rangle = \frac{\nu_2(\alpha_1, g^{-1}g^*, g^*)}{\nu_2(\alpha_2, g^{-1}g^*, g^*)}\,|g\alpha_1, g\alpha_2\rangle \tag{17}$$

The element g^* can be chosen arbitrarily but has to stay fixed. One needs to show that U^i indeed forms a linear representation on each lattice site and that the global action of $\otimes_i U^i$ leaves the wavefunction invariant. Chen et. al proved that this is the case, as long as $\nu_2(g_0, g_1, g_2)$ fulfills the cocycle relation Eq. 60. It is important to note that different choices for ν_2 do not always lead to different SPT phases. In fact, if two choices ν_2 and $\tilde{\nu}_2$ only differ by a 2-coboundary $\tilde{\nu}_2(g_0, g_1, g_2) = \nu_2(g_0, g_1, g_2)\frac{\mu_1(g_1,g_2)\mu_1(g_0,g_1)}{\mu_1(g_0,g_2)}$ they realize the same phase, as their states can be connected by a LU transformation [6]. We see that the different phases realized by the above construction can be labeled by elements of the second cohomology group $\mathcal{H}^2(G, U_T(1))$.

Let us take a closer look at the boundary of the 1-dimensional chain. The symmetry representation $U^i(g)$ acting on all the sites shown in Fig. 2b leads to

$$\otimes_i U^i(g) \left|\{\alpha_1, \gamma_2\}\right\rangle_B = \frac{\nu_2(\alpha_1, g^{-1}g^*, g^*)}{\nu_2(\gamma_2, g^{-1}g^*, g^*)} \left|\{g\alpha_1, g\gamma_2\}\right\rangle_B \tag{18}$$

where $\left|\{\alpha_1, \gamma_2\}\right\rangle_B$ denotes the state defined in Eq. 16 with boundary states α_1 and γ_2. One can easily tell, that the action of the symmetry on the boundary factorizes. We can therefore express the symmetry action as

$$[M(g) \otimes M(g)^*] \left|\{\alpha_1, \gamma_2\}\right\rangle_B \tag{19}$$

where $M(g)$ acts as $M(g)\left|\alpha_1\right\rangle = \nu_2(\alpha_1, g^{-1}g^*, g^*)\left|g\alpha_1\right\rangle$. Therefore the boundary states of our construction in 1+1 dimensions transform under a projective representation of the symmetry group.

In their derivation, Chen et al. make use of the geometrical interpretation of the cocycles ν_2. The cocycles are thereby identified with simplices and relations for phase factors are derived by comparing different complexes that are obtained by 'gluing' together several simplices. This is unfortunately not possible for our model, since a 3+1 dimensional system involves 4-cocycles which do no possess an easy graphical interpretation. Luckily, as the group $\mathbb{Z}_2^T = \{e, T\}$ is comparably small, we can explicitly check the needed relations by plugging in all possible combinations of group elements. Of course, our results will therefore only be applicable to SPT's for which the on-site symmetry is $\mathbb{Z}_2^T$.

Let us mention some things that apply to the 3+1 dimensional state: The partons inside of each effective site can be thought of to form a cube, the vertices of which we are going to label with numbers $a = 1, ..., 8$. We expect U^i to be of the general form

$$U^i(g)\left|\alpha_1, \alpha_2, ..., \alpha_8\right\rangle = \prod_{i=1}^{12} \nu_4(\alpha_{i_0}, \alpha_{i_1}, \alpha_{i_2}, g^{-1}, e)\left|g\alpha_1, ..., g\alpha_8\right\rangle \tag{20}$$

where $i_{0,1,2}$ can take values between 0 and 8. As the last two entries are the same for every ν_4 we sometimes use the notation $\nu_4(\alpha_{i_0}, \alpha_{i_1}, \alpha_{i_2}) \equiv \nu_4(\alpha_{i_0}, \alpha_{i_1}, \alpha_{i_2}, g^{-1}, e)$. One can now imagine $\nu_4(\alpha_{i_0}, \alpha_{i_1}, \alpha_{i_2})$ to lie on a triangle with oriented edges $\alpha_{i_2} \leftarrow \alpha_{i_0} \rightarrow \alpha_{i_1} \rightarrow \alpha_{i_2}$ (Fig. 3a). It also becomes clear why exactly 12 cocycles appear in Eq. 20, as this is the amount of triangles that is needed to cover the surface of the cube.

To obtain a final theory we still have to fix the $i_{0,1,2}$ for every value of i. This has to be done in a way that guarantees that U^i forms a linear representation and the wavefunction is invariant under the global action of U^i. Furthermore we require that the branching structure on the cube is consistent. We do not believe that this requirement is crucial but it certainly contributes to creating an manageable model.

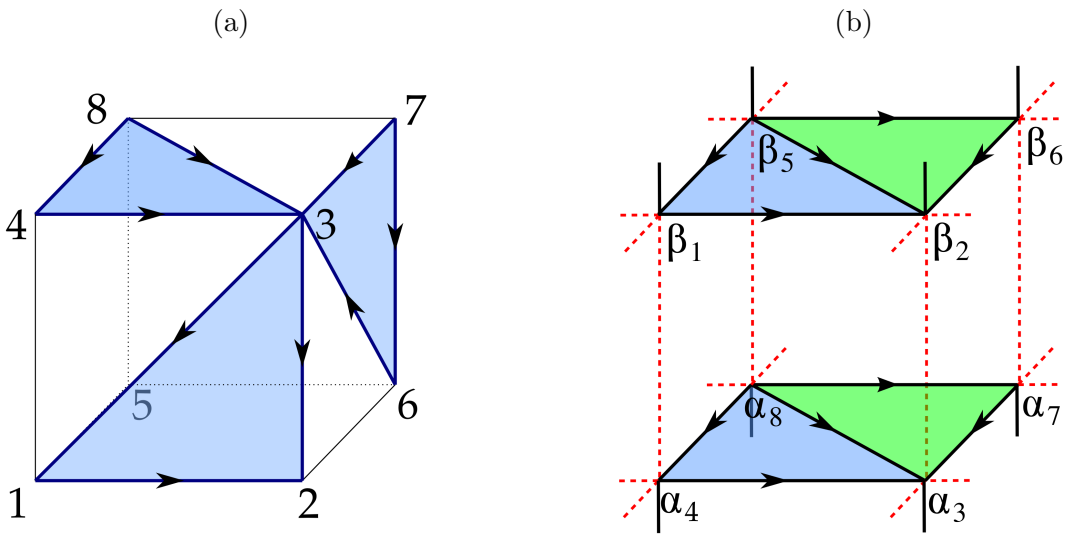

Figure 3: a) Labeling of the partons inside an effective site. The orientation of edges without arrows can be inferred by the orientation of edges with arrows. The orientation of edges on opposite sides of the cube is identical. b) Illustration for why triangles cancel out due to the entanglement structure. Partons connected by black solid lines belong to the same effective site. Partons connected by red dashed lines are entangled.

The requirement of invariance under a global symmetry transformation is easily fulfilled. All we have to do is make sure that the branching on opposite sides of the cube is identical. The entanglement structure of the canonical states leads to the fact that every triangle appears twice and therefore the phases cancel out (Fig. 3b). What is left is the trivial action of U^i on the wavefunction, which leaves the latter invariant due to the fact that all sites are maximally entangled and therefore transform as a singlet under the symmetry group.

Unfortunately we lack a similar understanding for the solution of the second requirement, namely that U^i forms a linear representation on every site i. We can, however, check numerically, which combinations for $i_{0,1,2}$ fulfill this requirement and which do not. It turns out that one finds multiple combinations. For our purposes, however, it is enough to pick one of them. Our choice is depicted in Fig. 3a, where the values for $i_{0,1,2}$ can be inferred from the orientation on the edges. The triangle in the front, for example, corresponds to $\nu_4(\alpha_3, \alpha_1, \alpha_2)$.

As the bulk of a SPT phase is believed to be trivial, we want to take a closer look at the theory induced on the surface. Therefore we truncate the system in the z -direction but maintain periodic boundary conditions in the other two directions. By doing so, we produce a layer of partons that initially are not entangled with their neighbors. We can impose, however, that the boundary structure be given by Fig. 2a, where now the bonds do no longer correspond to maximal entanglement but signal that two partons connected by them have to be in the same state - a somewhat less restrictive condition than the one used in the bulk. The reason we choose this structure is, on the one hand, if we

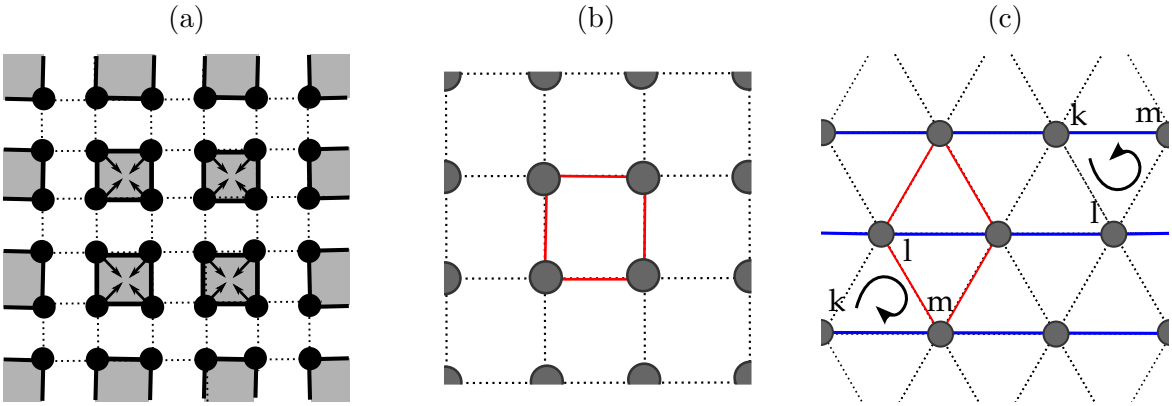

Figure 4: a) The original surface before "contracting" the bonds. b) Surface after the contraction. One new site is obtained by identifying four connected dots in a). c) New lattice obtained by rotating the original lattice (dashed) by 45 degrees, stretching and adding horizontal (blue) bonds.

imposed maximal entanglement on the surface, we would break time-reversal symmetry, on the other hand, if we did not impose any restrictions, the phase factor associated with symmetry transformations acting on the boundary would depend on the states inside of the bulk. This, however, is not desirable, as we wish to obtain a theory purely defined on the boundary.

We will now interpret the connected partons as the new effective sites on the surface. One can imagine that this can simply be obtained by 'contracting' (Fig. 4a) all the bonds. Furthermore, we rotate the square lattice by 45 degrees and add horizontal edges between the effective sites in order to obtain a triangular lattice. Going over to the new effective sites has the effect that $U^i(g)$ no longer acts locally, as the ν_4 involved in the associated phase factor depend on the states on several sites. More precisely, the symmetry transformation can be written as

$$\otimes_i U^i(g) \left|\phi\right\rangle = \prod_{\triangle,\triangledown} \nu_4(g_k, g_l, g_m) \left|g\phi\right\rangle \tag{21}$$

where $|\phi\rangle$ is the surface state and the product runs over all triangles (Fig. 4c). The non-locality of $U^i(g)$ is crucial and typical for the boundary of an SPT phase. It makes sure that we cannot simply gap out the surface without breaking T-reversal symmetry, an action that is forbidden for SPT phases.

We have now constructed a 3+1 dimensional state that realizes T-reversal SPT order. Our model is defined on a triangular lattice insofar as the phase factors that appear in the definition of the local symmetry transformation depend on spin-configurations that lie on triangles. So far, we have not implemented any specific Hamiltonian on the surface. Therefore, there is a massive degeneracy of states on the surface, as any wavefunction that is symmetric with respect to $\otimes_i U^i(g)$ can be seen as a ground state.

It is in principle possible to define any Hamiltonian on the surface that does not modify the bulk-theory and respects T-reversal symmetry (or rather its special representation defined in the section above). We believe that it should also be possible to find Hamiltonians that realize specific phases that are expected on the surface of a bosonic T-reversal SPT phase, in particular a state with $\mathcal{Z}_2$ topological order.

In Ch. 4, however, we will concentrate on another approach and try to connect the Chen-Gu construction to the O(4) non-linear sigma model by comparing spin-flip operations in both models.

2.5 Summary

In this chapter we have reviewed the construction for SPT phases developed by Chen et al. After defining LU operators, we have introduced the definition of SPT states as SRE entangled states protected by an on-site symmetry. SRE states can by definition be transformed to a direct product state by acting on them with LU operators. We have reviewed Chen et. al.'s construction of a 1D SPT chain and shown that its boundary states transform under a projective representation of the symmetry group.

As the paper by Chen et al. only defines constructions for (1+1) and (2+1)-dimensional systems, we have extended their results to (3+1)-dimensional systems with T-reversal symmetry and explicitly written down a theory for the (2+1)-dimensional boundary. This has partly been achieved by making use of the explicit struture of $\mathbb{Z}_2^T$, therefore our results are only applicable to systems with this on-site symmetry. The boundary theory is characterized by a non-local symmetry that is defined on triangles. This non-locality is typical for the boundary of an SPT phase and makes sure that it cannot be gapped out without breaking the symmetry.

3 Non-linear sigma model

3.1 Classification of SPT phases

In their paper, Bi et al. show that a classification of SPT phases similar to the one proposed by Chen et al., can be obtained by analyzing NLSM's with a topological term [3,6]. NLSM's are semiclassical field theories that are usually used to describe systems with long-range order. The Landau order parameter $\vec{n}$ plays the role of a fluctuating field and is normalized, so that $(\vec{n})^2 = 1$. This order parameter has a very intuitive understanding in O(3)-NLSM's, which describe 1+1 dimesional bosonic (spin) systems. The order parameter $\vec{n}$ thereby corresponds to the spin-polarization, i.e. to a point on the group-manifold of SU(2), which is the two-sphere S^2 [9]. In terms of the spin coherent states $|\vec{n}\rangle$, it can also be seen as the orientation of the expectation value $\langle\vec{n}|\,\vec{S}\,|\vec{n}\rangle = S\vec{n}$ [2]. The dynamical part defined as

$$S_0[\vec{n}] = \int d^d x d\tau \frac{1}{g}(\partial_\mu \vec{n})^2, \tag{22}$$

with imaginary time $\tau = it$, is able to describe many properties of long-range ordered systems, such as the excitation spectrum above the gap. Including the θ-term,

$$S_{\theta,1d}[\vec{n}] = \frac{i\theta}{\Omega_2} \int dx d\tau \epsilon_{abc} n^a \partial_x n^b \partial_\tau n^c, \tag{23}$$

$$S_{\theta,2d}[\vec{n}] = \frac{ik\theta}{\Omega_3} \int d^2 x d\tau \epsilon_{abcd} n^a \partial_x n^b \partial_y n^c \partial_\tau n^d, \tag{24}$$

$$S_{\theta,3d}[\vec{n}] = \frac{i\theta}{\Omega_4} \int d^3 x d\tau \epsilon_{abcde} n^a \partial_x n^b \partial_y n^c \partial_z n^d \partial_\tau n^e, \tag{25}$$

lets us access the topological properties of the system. If the system is now tuned to strong interactions $g >> 1$ the NLSM no longer provides a valid description of the system's dynamics. However, as the topolgical properties of the system are unchanged during this tuning process, the model can still be used to describe universal properties associated with SPT phases such as gapless edge modes [3].

It is worth noting that the maximum symmetry the order parameter can realize is given by O(d+2). This maximum symmetry, however, can always be broken down to the symmetry of interest. This is particularly easy, if O(d+2) is broken down to a discrete symmetry group, such as $\mathbb{Z}_2$, $\mathbb{Z}_2 \times \mathbb{Z}_2^T$ or $\mathbb{Z}_2 \times \mathbb{Z}_2$.

It has been shown by Bi et al. that the different SPT phases correspond to the different ways the symmetry transformation can be assigned to the order parameter so that the Lagrangian remains invariant for any value of θ. To give an example, in 3+1 dimensions the symmetry $\mathbb{Z}_2^A \times \mathbb{Z}_2^B$ has two independent realizations in term of the O(5)

order parameter $\vec{n}$ which are given by

$$\begin{aligned}
\text{Phase 1: } & \mathbb{Z}_2^A : n_{1,2} \to -n_{1,2}, n_a \to n_a (a = 3,4,5) \\
& \mathbb{Z}_2^B : n_1 \to n_1, n_a \to -n_a (a = 2,...,5) \\
\text{Phase 2: } & \mathbb{Z}_2^B : n_{1,2} \to -n_{1,2}, n_a \to n_a (a = 3,4,5) \\
& \mathbb{Z}_2^A : n_1 \to n_1, n_a \to -n_a (a = 2,...,5) \\
& .
\end{aligned}$$

We therefore obtain two "root"-phases. As both models can be realized with either $\theta = 0$ (the trivial case) or $\theta = 2\pi$, the classification of phases with symmetry $\mathbb{Z}_2 \times \mathbb{Z}_2$ is given by $(\mathbb{Z}_2)^2$, which corresponds to the fourth cohomology group $H^4(\mathbb{Z}_2 \times \mathbb{Z}_2, U(1)) = (\mathbb{Z}_2)^2$.

There is one rule for assigning transformation rules to the order parameter: No component can be left invariant by the action of the symmetry group G, otherwise one can turn on a Zeeman-term that polarizes $\vec{n}$ and opens an energy-gap for surface excitations without breaking G. This however is prohibited by the definition of SPT phases. One can easily convince oneself that this rule is indeed obeyed by the above transformations.

Note that the θ-term for 2+1 dimensional SPTs contains an integer k in front of the θ-angle. This is due to the fact that very often, for 2+1 dimensional systems, $\theta = 4k\pi$ and $\theta = 0$ do not describe the same phase. This has been proven by Bi et al. by coupling two systems at $\theta = 2\pi$ and driving the whole system from $\theta = 0$ to $\theta = 4\pi$. If this could not been done without closing the gap in the bulk, they concluded that both θ-angles necessarily describe two independent phases. Note that systems in 1+1 and 3+1 dimensions lack a k because they never realize independent phases at $\theta = 0$ and $\theta = 4\pi$.

Let us now illustrate the meaning of the topological θ-term by considering the case study of a spin-1 Heisenberg chain.

3.2 θ-term and the Heisenberg chain

In general the θ-term characterizes the topological properties of a mapping $n : S^{d+1} \to S^{d+1}$. One of these topological properties is the homotopy group $\pi_{d+1}(S^{d+1}) = \mathbb{Z}$. Starting with a flat spacetime manifold in d+1 dimensions, we assume that all points at infinity can be identified as one single point and that we can therefore compactify the spacetime manifold to a (d+1)-sphere, S^{d+1}. The order parameter of a O(d+2) NLSM has d+2 components which are normalized so that $\sum_{i=0}^{d+2}(n^i)^2 = 1$. It therefore describes points lying on the manifold S^{d+1}. The θ-term can be used to measure how often the spacetime-configurations of $\vec{n}$ wrap around the unit d+1-sphere. We will refer to this wrapping number as $\mathcal{Q} \in \pi_{d+1}(S^{d+1})$.

Let ω be a volume(top-dimensional)-form on a compact d+1 dimensional manifold.

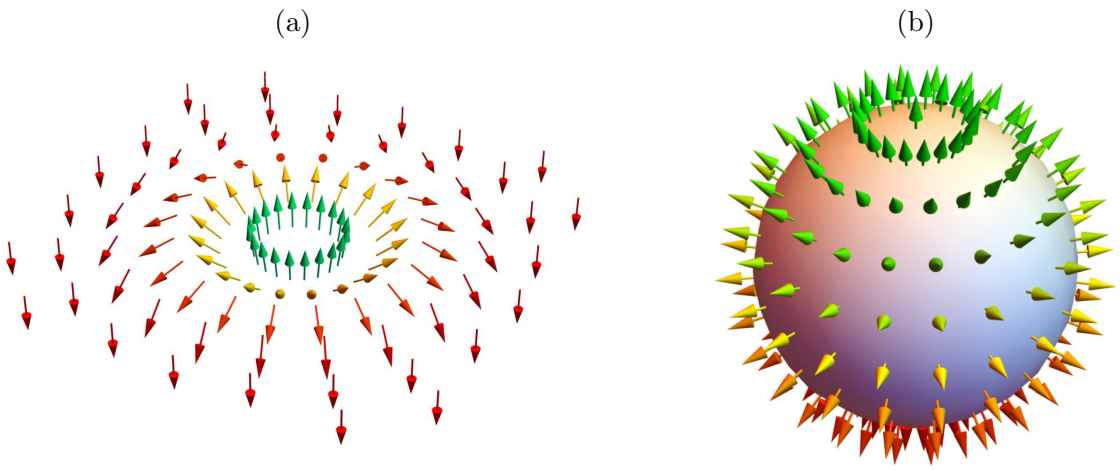

Figure 5: a) Configuration in the x-τ-plane that realizes a skyrmion. b) Compactifying spacetime, one can tell that the winding number associated with the skyrmion configuration $\mathcal{Q} = 1$.

Further, let $\vec{n}$ be a field that maps from S^{d+1} to S^{d+1}. This implies that $n^a : S^{d+1} \to \mathbb{R}$. The θ-term can now be written as

$$S_\theta = i\theta\mathcal{Q} = i\theta \int \vec{n}^*\omega \tag{26}$$

where $\vec{n}^*\omega$ denotes the pullback of the volume-form induced by the function $\vec{n}$. The topological action, does not influence the equations of motion and is invariant under infinitesimal variations of the field-configuration [2]. The coordinate-free representation of the θ-term is very compact, in some cases it might however be to abstract for actual computations. Two other representations are easily obtained by Eq. 26, and are given by

$$S_{\theta,d} = \frac{i\theta}{\Omega_{d+1}} \int \epsilon_{a_1 a_2 .. a_{d+2}} n^{a_1} \wedge dn^{a_2} \wedge dn^{a_3} \wedge ... \wedge dn^{a_{d+2}} \tag{27}$$

and

$$S_{\theta,d} = \frac{i\theta}{\Omega_{d+1}} \int d^d x d\tau \frac{1}{(d+1)!} \epsilon^{\mu_1 \mu_2 ... \mu_{d+1}} \epsilon_{a_1 a_2 .. a_{d+2}} n^{a_1} \partial_{\mu_1} n^{a_2} \partial_{\mu_2} dn^{a_3} ... \partial_{\mu_{d+1}} n^{a_{d+2}} \tag{28}$$

for d+1 dimensional spacetime, where $\wedge$ is the wedge-product and ϵ the Levi-Civita symbol. It is easy to convince oneself that the integrand in Eq. 27 is indeed a top-dimensional form on S^{d+1} and the integral therefore well-defined.

In one dimensional systems, the spin-1 Heisenberg chain is a prominent and well-understood example for an SPT phase and is described by a NLSM with θ-term at $\theta = 2\pi$

$$S = \int dx d\tau \frac{1}{g} (\partial_\mu \vec{n})^2 + \frac{i2\pi}{\Omega_2} \int d^2 x d\tau \epsilon_{abc} n^a \partial_x n^b \partial_\tau n^c \tag{29}$$

Let us, for now, concentrate on the topological part of the action. As before, the θ-term attaches a phase to every spin-configuration in spacetime depending on its winding number $\mathcal{Q}$. It is instructive to interpret the imaginary time τ as a second euclidean dimension. Consider for example the configuration shown in Fig. 5. The configuration in 1+1 dimensional spacetime is referred to as a skyrmion. To obtain the winding number, it is useful to compactify spacetime. Note that the spin direction on every point on the border of the depicted spacetime is the same. This is also meant to be the case for every possible point at infinity. We can therefore identify all these 'infinities' and obtain a spacetime that is compactified on a 2-sphere. It is easy to see that, going around the 2-sphere once, also the 2-sphere traced out by the spin configuration is covered once. Therefore the winding number of the shown configuration is 1.

The contribution of the topological action is usually interpreted as a phase factor $\exp(-S_\theta) = \exp(-i\theta\mathcal{Q})$ associated with every instanton event in spacetime. One could therefore think that $\theta = 2\pi$ and $\theta = 0$ describe the same physical system. This is however only true if the system is defined on a compact spacetime manifold. As soon as we include boundaries in our system, even $\theta = 2\pi$ causes non-trivial effects as we will see below.

However, to describe the boundary of a system we have to go over from the θ-term to another kind of topological action, namely the Wess-Zumino-Witten(WZW)-term [22].

3.3 Boundaries and the WZW-term

To derive a surface theory, we follow the discussion by Vishwanath and and Senthil [20]. Let us consider a 3+1 dimensional SPT state, which is described by a O(5) NLSM. Instead of constructing a boundary between a state where $\theta = 2\pi$ and the vacuum, we can consider a domain wall between $\theta = 2\pi$ and $\theta = 0$. To do so, let us enlarge our original 5-component vector $\vec{n}$ by an additional component so that

$$\vec{\phi} = \begin{pmatrix} \cos(\alpha) \\ \vec{n}\sin(\alpha) \end{pmatrix} \tag{30}$$

Where $\vec{\phi}$ is again normalized to 1 but no longer maps from S^4 to S^4 but $\phi : S^4 \to S^5$. It is no longer possible to describe the topological properties of $\vec{\phi}$ with a θ-term. One rather has to extend the spacetime from S^4 to its inside, given by the 5-ball B_5. The new topological term on can write down to obtain a winding number for the mapping $\phi : B_5 \to S^5$ is given by

$$S_{WZW}[\phi] = \frac{i2\pi}{\Omega_5} \int_{x,\tau} \int_0^1 du\ \epsilon_{abcdef}\ \phi^a \partial_x \phi^b \partial_y \phi^c \partial_z \phi^d \partial_\tau \phi^e \partial_u \phi^f . \tag{31}$$

Of course we also have to extend $\vec{\phi}$ into the 5-ball. This should be done in a way so that

the order parameter is "frozen-out" for $u = 0$ (the middle of the ball). One can prove that the way we choose to interpolate between given boundary conditions into the ball does not affect the topological phase given by the WZW term. One possible extension is given by

$$\vec{\phi} = \begin{pmatrix} \cos\alpha(u) \\ \vec{n}\sin\alpha(u) \end{pmatrix}, \tag{32}$$

where $\alpha(0) = 0$, $\alpha(1) = \alpha$, $\alpha(u)$ is independent of $(\vec{x}, \tau)$ and $\vec{n}$ is independent of u. Plugging in Eq. 32 into Eq. 31 one can integrate out u and obtain a θ-term. The topological angle, however, now depends on how we chose the value of α. Starting with Eq. 31 we arrive at

$$\begin{aligned} S_{WZW}[\vec{\phi}] &= \frac{2}{\pi^2}\int_{\vec{x},\tau}\int_0^1 du \frac{d\alpha}{du}\{\epsilon_{abcde1}\,(-\sin^6\alpha)\, n^a\partial_x n^b\partial_y n^c\partial_z n^d\partial_\tau n^e \\ &\qquad \epsilon_{1bcdef}\,\sin^4\alpha\,\cos^2\alpha\, n^f\partial_x n^b\partial_y n^c\partial_z n^d\partial_\tau n^e\} \\ &= \frac{2}{\pi^2}\int_{\vec{x},\tau}\int_0^\alpha d\alpha'\epsilon_{1abcde}\,\sin^4\alpha'\, n^a\partial_x n^b\partial_y n^c\partial_z n^d\partial_\tau n^e. \end{aligned} \tag{33}$$

After integrating out $\alpha'(u)$, we obtain an O(5) θ-term (Eq. 25) with topological angle

$$\theta = \frac{16}{3}\int_0^\alpha d\alpha'\sin^4\alpha', \tag{34}$$

which leads to $\theta = 0$ for $\alpha = 0$ and $\theta = 2\pi$ for $\alpha = \pi$. This means that if we choose the extension given by Eq. 32 and set $\alpha = \pi$, then the WZW-term is equivalent to a θ-term at $\theta = 2\pi$. In fact, this result can be generalized to arbitrary dimensions. Consider a O(d+2) NLSM with WZW-term, and an order parameter given by

$$\vec{\phi}_{d+3} = \begin{pmatrix} \cos\alpha(u) \\ \vec{n}_{d+2}\sin\alpha(u) \end{pmatrix}, \tag{35}$$

where now $\vec{n}_{d+2}$ is a dynamical (n+2)-dimensional order parameter and $\vec{\phi}_{d+3}$ is its extension into B_{d+2}. As before $\alpha(0) = 0$ and $\alpha(1) = \alpha$. Setting $\alpha = \pi$ and integrating out u leads to a θ-term, whose θ-angle is given by

$$\frac{\theta}{2\pi} = \frac{\Omega_{d+1}}{\Omega_{d+2}}\int_0^\pi d\alpha'(\sin\alpha)^{d+1} = 1. \tag{36}$$

Similarly,

$$\frac{\theta}{2\pi} = \frac{\Omega_{d+1}}{\Omega_{d+2}}\int_0^{\pi/2} d\alpha'(\sin\alpha)^{d+1} = \frac{1}{2}. \tag{37}$$

for $\alpha = \pi/2$.

To model a domain wall between both θ-angles, say in the x-y-plane, we can make α

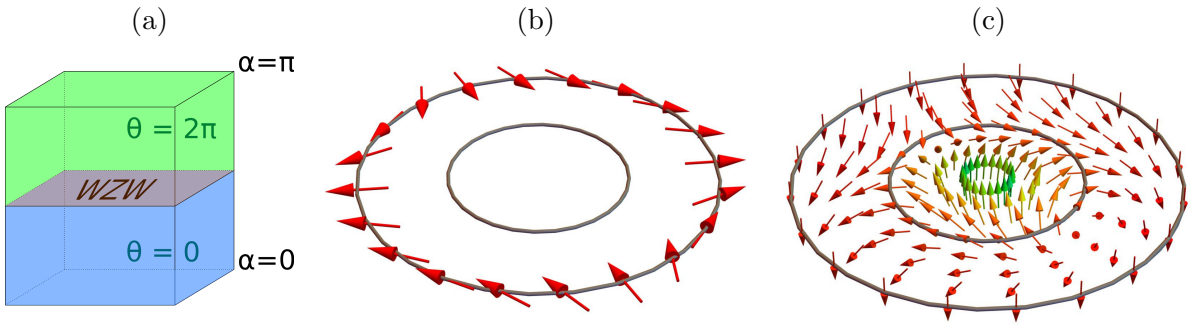

Figure 6: a) Domain wall between a state with $\theta = 0$ and a state with $\theta = 2\pi$. The bulk is described by a θ-term whereas the boundary (domain-wall) is described by a WZW-term.b),c) Spin-configuration on S^1 and its extension into B_2. The extension is chosen, so that the WZW-term for B_2 corresponds to a θ-term with $\theta = 2\pi$ on S^1. The rings mark $u = 1/2$ and $u = 1$.

depend on the coordinate z, $\alpha \to \alpha(z)$. We impose

$$\alpha(z \to -\infty) = 0 \qquad\qquad \alpha(z \to \infty) = \pi \tag{38}$$

which corresponds to

$$\theta(z \to -\infty) = 0 \qquad\qquad \theta(z \to \infty) = 2\pi. \tag{39}$$

Furthermore we want the derivative $d\alpha/dz$ to be localized around $z = 0$, where the domain wall is supposed to be located (Fig. 6a). As our aim is to integrate out z in Eq. 31 it is convenient to use a different interpolation for the order parameter $\vec{\phi}$, which is given by

$$\vec{\phi} = \begin{pmatrix} \cos\alpha(z) \\ \vec{n}(\vec{x},\tau,u)\sin\alpha(z) \end{pmatrix}, \tag{40}$$

where now $\alpha(z)$ is independent of (x, y, τ, u) and $\vec{n}(\vec{x},\tau,0) = \vec{n}_0$, $\vec{n}(\vec{x},\tau,1) = \vec{n}(\vec{x},\tau)$. Again, plugging Eq. 40 into Eq. 31 we obtain,

$$S_{WZW} = \frac{2}{\pi^2}\int_{x,y,\tau}\int_0^1 du \int_{-\infty}^{\infty} dz\, \epsilon_{1abcde}\,\frac{d\alpha}{dz}\,\sin^4\alpha\, n^a\partial_x n^b\partial_y n^c\partial_\tau n^d\partial_u n^e. \tag{41}$$

Making use of the fact that $d\alpha/dz$ is localized at $z = 0$, we can replace the field $\vec{n}(\vec{x},\tau,u)$ by $\vec{n}(x, y, z = 0, \tau, u)$ and perform the integration over z. The result is a level-1 WZW term for the boundary at $z = 0$:

$$S_{WZW} = \frac{2\pi}{\Omega_4}\int_{x,y,\tau}\int_0^1 du\,\epsilon_{abcde}\, n^a\partial_x n^b\partial_y n^c\partial_\tau n^d\partial_u n^e. \tag{42}$$

Our results can be generalized to arbitrary dimensions. Indeed it turns out that if a

(d+1)-dimensional system is described by a O(d+2) NLSM with a θ-term at $\theta = 2\pi$, then its (d-1+1)-dimensional boundary can be described by a O(d+2) NLSM with a level-1 WZW-term.

Let us take a closer look at the boundary of a 1+1 dimensional spin-1 Heisenberg chain. As stated above, the bulk can be described by a O(3) NLSM with $\theta = 2\pi$, therefore the 0+1 boundary, which corresponds to a point, is described by a O(3) NLSM with a WZW-term

$$S_b = \int d\tau \frac{1}{g}(\partial_\tau \vec{n})^2 + \int d\tau du \frac{i2\pi}{\Omega_2} \epsilon_{abc} n^a \partial_\tau n^b \partial_u n^c., \tag{43}$$

where $\vec{n}(\tau, u)$ is again extended into B_2. The action given by Eq. 43 describes a point particle moving on a sphere S^2 threaded by a magnetic flux of 2π (measured in unit flux) [3]. As expected for the boundary of a SPT, the ground state for this problem is two fold degenerate. The wavefunction doublet is given by

$$\psi_1 = \cos(\vartheta/2) e^{i\phi/2} \qquad \psi_2 = \sin(\vartheta/2) e^{-i\phi/2} \tag{44}$$

where $\vec{n}$ is parametrized by spherical coordinates $\vec{n} = (\sin\vartheta\cos\phi, \sin\vartheta\sin\phi, \cos\vartheta)$. Suppose the SPT-phase is protected by T-reversal symmetry, which acts as $\vec{n} \to -\vec{n}$. Then in terms of the spherical coordinates we can write the action of T as $\phi \to \phi$ and $\theta \to \theta + \pi$. Therefore the doublet $|\psi\rangle = (\psi_1, \psi_2)^T$ transforms as $|\psi\rangle \to i\sigma^y |\psi\rangle$ where σ^y is the standard Pauli-matrix with imaginary entries.

It is easy to see that $|\psi\rangle$ transforms as a Kramer's doublet under T-reversal as $T^2 : |\psi\rangle \to (i\sigma^y)^2 |\psi\rangle = -|\psi\rangle$. This corresponds to another property of 1+1d SPT phases, namely that their boundary states transform projectively under the action of the protecting symmetry.

Now let us go back to our 3+1 dimensional SPT protected by T-reversal. The boundary theory is by Eq. 42, where $\vec{n}$ transforms as $\vec{n} \to -\vec{n}$ under T-reversal. Let us change the notation and replace $\vec{n}$ by $\vec{\phi}$, keeping in mind that this order parameter is extended from the spacetime manifold S^3 into B_4. This means that there are some unphysical redundancies in the order parameter $\vec{\phi}$. Now assume that the extension is given by

$$\vec{\phi} = \begin{pmatrix} \cos\alpha(u)\phi_0 \\ \vec{n}(\vec{x}, \tau)\sin\alpha(u) \end{pmatrix}, \tag{45}$$

where $\phi_0 = \pm 1$ is an Ising-like parameter and $\alpha(u)$ is independent of $\vec{x} = (x, y)^T$ and τ. Time-reversal invariance implies $\langle\phi_1\rangle = 0$ for the physical subspace of B_4. We can therefore set $\alpha(0) = 0$ and $\alpha(1) = \pi/2$, which implies that $\vec{\phi}(\vec{x}, \tau, 0) = (\phi_0, \vec{0})^T$ and $\vec{\phi}(\vec{x}, \tau, 1) = (0, \vec{n})^T$ [3, 23]. With the help of Eq. 37, we can now integrate out u. The

reduced action is given by an O(4) NLSM with θ-term:

$$S_{\text{reduced}} = \int d^2x d\tau \left\{ \frac{1}{g} (d_\mu \vec{n})^2 + \frac{i\pi}{\Omega_3} \epsilon_{abcd} n^a \partial_x n^b \partial_y n^c \partial_\tau n^d \right\}. \tag{46}$$

The topological angle $\theta = \pi$ implies that, even though the orginal θ-term for the 3+1 dimensional system did not influence any dynamics in the bulk, it induces an effective surface theory for which instanton events are dressed with a topological phase $\exp(i\pi\mathcal{Q})$, which is no longer trivial. This, however, is exactly what we expected for SPT phases, namely that the bulk is a trivial insulator and has therefore no topological properties. And further, that all interesting phenomena, such as (topological) degeneracies and gapless states, occur on the boundary. Furthermore, for the boundary theory $\theta = \pi$ is protected by time-reversal symmetry. This stands in contrast to the bulk, which is by definition T-reversal invariant for any value of θ.

4 Connection between NLSM and Chen-Gu construction

4.1 Outline

The Chen-Gu construction introduced in section 2 gives an explanation for why SRE topological phases in $1+d$ dimensions that are protected by an on-site symmetry G can be labeled by elements of the cohomology group $\mathcal{H}^{1+d}[G, U_T(1)]$. However it is merely defined by the action of G on the wavefunction and lacks an implementation of a dynamical Hamiltonian, which would allow for a notion of the system's energy spectrum. Especially on the surface, it would be desirable to construct a Hamiltonian that realizes the typical phases expected in systems with SPT order.

One step towards a deeper understanding and an easier accessibility of the Chen-Gu construction is to connect it to other well-known models describing SPT phases. To realize such a connection we compare the action of spin-flip operators in the NLSM to that in the Chen-Gu construction.

One difficulty we have to deal with is the obvious fact that the former model is defined in the continuum whereas the latter exists on a discrete lattice. This issue can be resolved by continuously interpolating spin configurations between the lattice sites by a procedure described below. Also the question of how a spin-flip operator can be implemented in the path-integral formalism arises. As in the case of interpolating between the lattice sites we continuously connect the time slices before and after the spin-flip, leaving us with a spin configuration in 2+1 dimensional spacetime.

Having defined spin-flip operators in both models, we can compare their properties such as the commutation relations of neighboring spin-flips. We expect these relations to be encoded in the θ-term of the NLSM.

4.2 Chen-Gu construction on a triangular lattice

As the action of the on-site symmetry G is defined through cocycles which "lie" on triangles (Eq. 21), it is natural to think of our model in terms of a triangular lattice. By rotating the original lattice by 45 degrees, we can distinguish between triangles pointing upwards and triangles pointing downwards (Fig. 4c). We can now introduce an operator σ_r^x that flips the spin on site r. We note that the triangles that site r is part of, form a hexagon. The spin configuration on the boundary of the hexagon is denoted by $|h\rangle \in \mathcal{H} = \bigotimes_{i=1}^{6} \mathbb{C}^2$. The total spin configuration is given by $|c\rangle \in \mathcal{H} = \bigotimes_{i=1}^{N} \mathbb{C}^2$ where N is the number of sites in our system. A connection to the construction in Ch. 2 can be obtained by identifying $e \hat{=} \uparrow$ and $T \hat{=} \downarrow$. We use the notation $|c\rangle \equiv |r, h, rest\rangle \equiv |r, h\rangle$

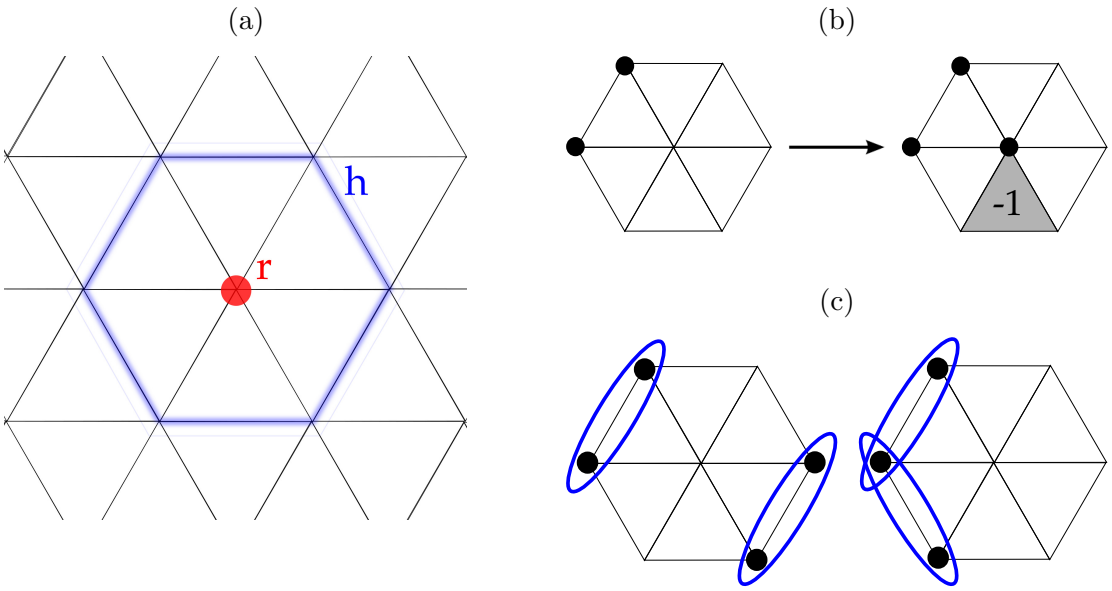

Figure 7: a) Different areas used in the wavefunction of the spin configuration. b) Example for the evaluation of the eigenvalues of $\hat{\chi}_r$: Black circles denote sites occupied by down spins, sites without a dot are occupied by spins pointing upwards. Flipping the spin (denoted by arrow) on the central site adds a triangular plaquette (shaded gray), which corresponds to an additional phase factor of -1 when acting with T on the system. The eigenvalue of $\hat{\chi}_r$ for the above configuration is therefore -1. c) Illustration of nearest neighbor spin-down bonds. In both cases $n = 2$.

(Fig. 7a) so that the spin-flip operator acts as

$$\sigma_r^x |r, h\rangle = |\bar{r}, h\rangle \tag{47}$$

where $|\bar{\uparrow}\rangle = |\downarrow\rangle$ and $|\bar{\downarrow}\rangle = |\uparrow\rangle$. Clearly σ_r^x does not always commute with the time-reversal operator $\hat{T} \equiv \otimes_i U^i(T)$. One can construct an operator $\tilde{\sigma}_r^x$ which commutes with $\hat{T}$, however this operator is no longer necessarily hermitian or squares to one.

To find such an operator, it is instructive to investigate the commutation relations between σ_r^x and $\hat{T}$ for certain spin configurations. We define the operator $\hat{\chi}_r$ so that

$$\hat{T}\sigma_r^x = \sigma_r^x \hat{T}\hat{\chi}_r. \tag{48}$$

This operator is diagonal in the spin basis and its eigenvalues are either plus or minus unity, signaling whether $\hat{T}$ and σ_r^x commute or anticommute. It is clear that the eigenvalue of $\hat{\chi}_r$ can only depend on the configuration of the hexagon encircling the site r. By going through all the possible configurations (Fig. 7b) one finds that

$$\hat{\chi}_r |r, h\rangle = (-1)^n |r, h\rangle, \tag{49}$$

where n is the number of nearest neighbor down spins on the hexagon h (Fig. 7c). It is obvious that $[\hat{T}, \hat{\chi}_r] = 0$. Equipped with this information, we can modify the spin flip operator by $\hat{\alpha}_r$. We impose that this operator be hermitian and that it be diagonal in the spin basis (we only want to flip the spin once). We also want $\hat{\alpha}$ to be as local as possible, and therefore make its eigenvalues $\hat{\alpha}_r|r,h\rangle = \alpha(r,h)|r,h\rangle$ depend only on the configuration on the hexagon and on site r. Imposing that $\hat{T}$ and $\tilde{\sigma}_r^x = \sigma_r^x\hat{\alpha}$ commute leads to

$$\begin{aligned}
[\hat{T}, \tilde{\sigma}_r^x] &= 0 \\
(\hat{T}\sigma_r^x\hat{\alpha}_r - \sigma_r^x\hat{\alpha}_r\hat{T})|r,h\rangle &= 0 \\
(\sigma_r^x\hat{T}\hat{\chi}_r\hat{\alpha}_r - \sigma_r^x\hat{\alpha}_r\hat{T})|r,h\rangle &= 0 \\
\chi(h)\alpha(r,h) - \alpha(\bar{r},\bar{h}) &= 0 \\
\chi(h) &= \alpha(\bar{r},\bar{h})/\alpha(r,h)
\end{aligned} \tag{50}$$

The most symmetric way to solve Eq. 50 is given by

$$\hat{\alpha}_r = \frac{1}{2}(1+\hat{\chi}_r) - \frac{1}{2}\sigma_r^z(1-\hat{\chi}_r) \tag{51}$$

where σ_r^z is the standard Pauli-matrix that is diagonal in the spin basis. As mentioned before, the newly defined operator $\tilde{\sigma}_r^x = \sigma_r^x\hat{\alpha}_r$ ceases to square to unity, when acting on arbitrary spin configurations. More precisely

$$(\tilde{\sigma}_r^x)^2|r,h\rangle = \chi(h)|r,h\rangle. \tag{52}$$

The operator as a whole neither is hermitian nor antihermitian. Acting on a spin configuration, however, it seems to be hermitian for configurations on which it squares to unity and antihermitian where it squares to minus unity. Furthermore, by modifying the Pauli-matrix σ_r^y by

$$\tilde{\sigma}_r^y = \frac{1}{2}\sigma_r^y\left[(1+\hat{\chi}_r) - (1-\hat{\chi}_r)\sigma_r^z\right] \tag{53}$$

and by identifying $\sigma_r^z = \tilde{\sigma}_r^z$, we can recover the standard equal-space commutator for Pauli-matrices given by

$$\left[\tilde{\sigma}_r^a, \tilde{\sigma}_r^b\right] = 2i\epsilon^{abc}\tilde{\sigma}_r^c \tag{54}$$

We can now take a closer look on the commutation relations for spin-flips on nearest neighbor sites and define the operator $\hat{\gamma}$ by $\tilde{\sigma}_r^x\tilde{\sigma}_{r'}^x = \tilde{\sigma}_{r'}^x\tilde{\sigma}_r^x\hat{\gamma}$. It is obvious that the eigenvalue of $\hat{\gamma}$ can only depend on the spin configuration on the intersection between the two hexagons encircling r and r'. On the edges of this diamond lie the sites which we label as r,r', A and B (see Fig. 8a). Multiplying both sides of the equation above by

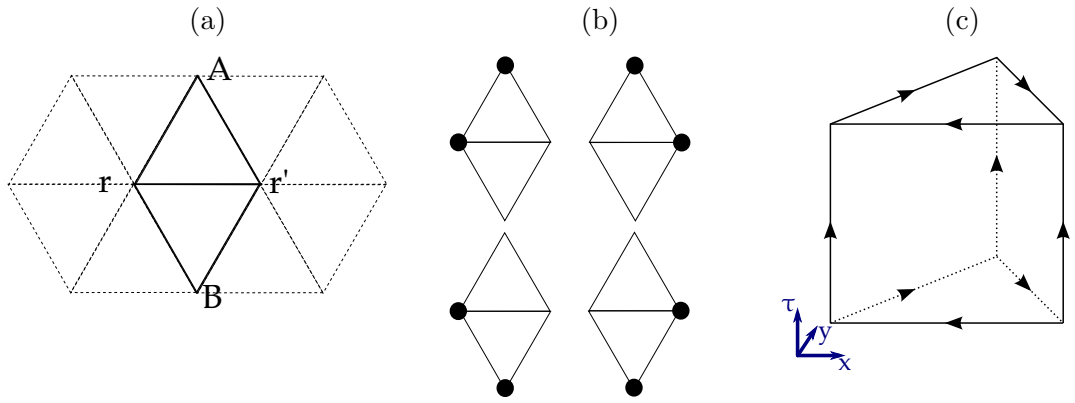

Figure 8: a) Labeling of the sites on which the eigenvalue of $\hat{\gamma}_r$ depends. b) All the spin configurations for which $\hat{\gamma}_r$ has eigenvalue -1. The different configurations are related by two mirror symmetries. c) Prism in 2+1 dimensional euclidean spacetime with oriented edges. Lattice sites that differ regarding their τ-coordinate are to be interpreted as events in spacetime before and after a certain spin-flip

the state $|r, h\rangle$ leads to

$$\gamma(r, r', A, B) = \frac{\alpha(r, h(\bar{r}'))\alpha(r', h')}{\alpha(r', h'(\bar{r}))\alpha(r, h)} \tag{55}$$

where $h(r')$ denotes the spin configuration on the hexagon around r with the spin on site r' flipped. The following observations lead to an expression for $\gamma(r, r', A, B)$:

1. $\chi(h) \neq \chi(h(\bar{r}'))$ only if the spin on A **or** B (not on both) is pointing downwards
2. The same applies to $\chi(h')$ and $\chi(h'(\bar{r}))$
3. If the above applies, $\gamma(r, r', A, B) = -1$ if the spins on r and r' point in opposite directions
4. $\gamma(r, r', A, B) = 1$ for all other cases

This can be summarized as

$$\gamma(r, r', A, B) = \begin{cases} \sigma_r^z \sigma_{r'}^z & \text{if } \sigma_A^z \sigma_B^z = -1 \\ 1 & \text{if } \sigma_A^z \sigma_B^z = 1 \end{cases}$$

where σ^z is the typical Pauli matrix diagonal in the spin basis, and the operators above should be replaced by their eigenvalues when acting on a spin configuration. The only configurations for which $\gamma(r, r', A, B) = -1$ are shown in Fig. 8b. For those who feel uncomfortable with an anti-hermitian spin-flip operator, Appendix B provides an alternative approach to obtaining the sign-factors of interest.

We can now move on to the NLSM and try to find spin flip operators that obey the same relations as $\tilde{\sigma}_r^x$.

4.3 Spin flip operators in the NLSM

To compare a lattice model to a continuum theory like the NLSM, we need to fix rules on how to interpolate spin configurations between the lattice sites.

Remembering that the vector $\vec{n}$ in our O(4) NLSM has 4 components and is normalized so that $|\vec{n}| = 1$ we can identify $|\uparrow\rangle : \vec{n} = (0,0,1,0)^T$ and $|\downarrow\rangle : \vec{n} = (0,0,-1,0)^T$. As the vector $\vec{n}$ describes points lying on S^3 it is illuminating to parametrize it by hyperspherical coordinates with unit radius :

$$\vec{n} = (\cos\psi, \sin\psi\cos\theta, \sin\psi\sin\theta\cos\phi, \sin\psi\sin\theta\sin\phi)^T$$

where now $|\uparrow\rangle : (\psi,\theta,\phi) = (0,0,0)$ and $|\uparrow\rangle : (\psi,\theta,\phi) = (0,0,\pi)$.

For our later calculations it turns out to be convenient to consider prisms, that is 3-dimensional objects with two triangular and three rectangular surfaces, as our basic building blocks (Fig. 8c). The third dimension thereby corresponds to imaginary (euclidean) time and can be treated as a spatial dimension.

Interpolating on edges. First, let us fix a rule for interpolating between two neighboring sites lying on the vertices of the prism. It is clear that, in order to define these rules we have to fix an orientation on the edges. This can be done arbitrarily, but once chosen it has to remain fixed for all configurations.

As long as we only consider configurations on the edges, we can restrict ourselves to $\vec{n}$'s lying in the U(1) subspace of O(4). In other words the vector $\vec{n}$ lies on the circle S^1 parametrized by the angle ϕ with $\psi, \theta = \text{const.} = 0$. We can now write down the following rules:

1. $|\uparrow\rangle \to |\uparrow\rangle : \psi = \theta = \phi = 0$
2. $|\downarrow\rangle \to |\downarrow\rangle : \psi = \theta = 0, \phi = \pi$
3. $|\uparrow\rangle \to |\downarrow\rangle : \psi = \theta = 0, \phi : 0 \to \pi$
4. $|\downarrow\rangle \to |\uparrow\rangle : \psi = \theta = 0, \phi : \pi \to 2\pi$

It is worth noting that by fixing rule 3 we automatically fix rule 4 as they are related by time reversal. Also, it is of no importance how the transition from $|\uparrow\rangle$ to $|\downarrow\rangle$ (or vice versa) is implemented, as long as $\vec{n}$ only covers the upper (lower) half of S^1 (Fig. 9a). One possible implementation however is given by $\vec{n} = (0,0,\cos(\lambda\pi),\sin(\lambda\pi))^T$ where $\lambda \in [0,1]$. All other implementations are equal to this one in the topological sense.

Interpolating on surfaces. Having fixed the configuration on the edges, we can now interpolate onto surfaces between the edges. However, before doing so, it is important

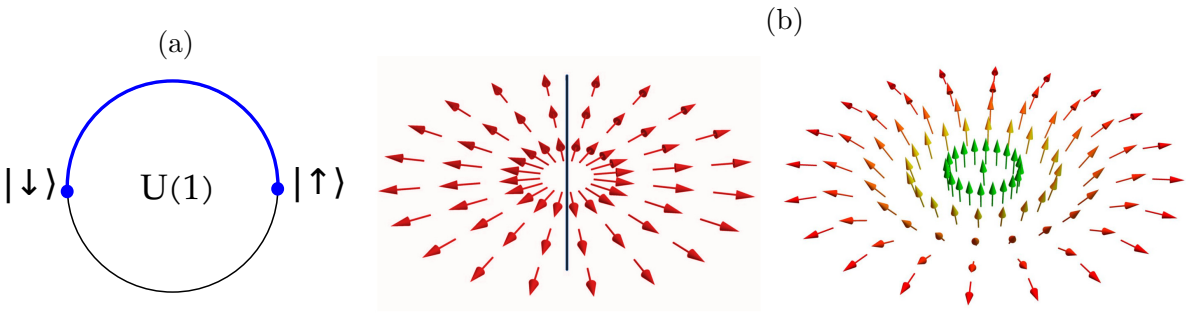

Figure 9: a) The interpolation from $|\uparrow\rangle$ to $|\downarrow\rangle$ covers the upper half of S^1. b) Interpolating configurations with winding number $\nu_1 = 1$ necessarily binds a vortex (blue line) if $\vec{n}$ is restricted to U(1). The vortex can be avoided by covering a hemisphere of O(3) $\cong$ SU(2) $\cong S^2$ (depicted on the right)

to take a closer look at the winding number ν_1 of the configuration on the surrounding edges: For $\nu_1 = 0$ the configuration can be continued trivially onto the surface, i.e. $\vec{n}$ remains restricted to U(1). However, if $\nu_1 = 1$ this necessarily binds a vortex. A vortex, being a discontinuity in the spin configuration, has to be avoided, and it is therefore necessary to introduce an additional rule stating that, if $\nu_1 = 1$, one has to interpolate onto the surface by extending $\vec{n}$ into the SU(2) subspace of O(4). That way, a vortex can be omitted and a smooth spin configuration achieved.

The rules associated with the extension onto the two-sphere S^2 again have to respect time-reversal symmetry. Therefore, by fixing the convention that spin configurations with mostly up-spins on the vertices have to be extended over the upper hemisphere of S^2 (Fig. 9b), we automatically make sure that configurations with mostly down-spins on the vertices are extended over the lower hemisphere. This definition is unique, as on a triangle with three vertices, there is always a dominating spin direction and on a rectangle with four vertices only certain configurations, in particular configurations without an equal number of up- and down-spins, bind a vortex.

Interpolating in the bulk. To interpolate from the configuration on the surfaces into the bulk, we use a similar reasoning as above. Again we look for configurations which bind a vortex, and extend $\vec{n}$ to the full O(4) manifold. As above, we can define a winding number ν_2, only this time the winding number characterizes a mapping $S^2 \to S^2$ (from the surface of the prism to the manifold of O(3)) instead of $S^1 \to S^1$. Both mappings have a well defined winding number as $\pi_n(S^n) = \mathbb{Z}$.

Again, we introduce the rule that if the $\nu_2 = 0$ the configuration is to be continued trivially into the bulk, i.e. $\vec{n}$ stays restricted to the O(3) subspace. However, if $\nu_2 = 1$, we interpolate by covering the upper (lower) hemisphere of S^3 in order to avoid a vortex. Of course this rule lacks a graphical description but the argumentation is exactly the same as above. Note that, just as S^1 is the boundary of a hemisphere of S^2, S^2 is the boundary

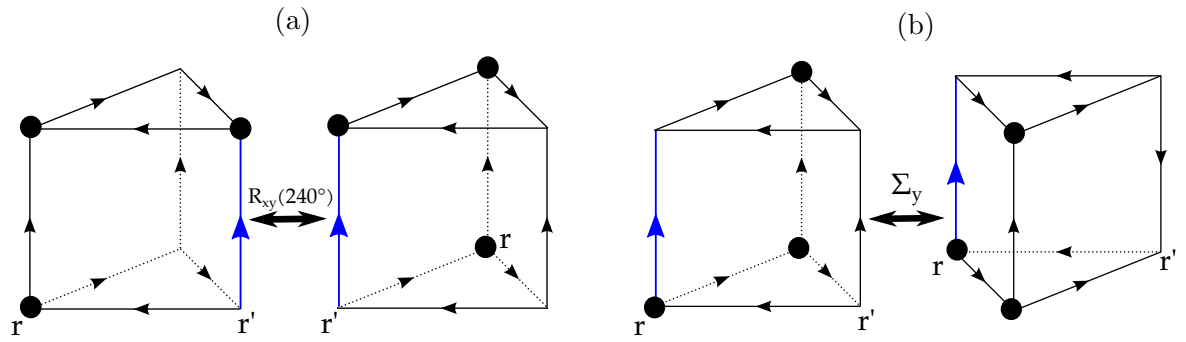

Figure 10: a) Two spin configurations related by a 240 degree rotation in the x-y-plane. Both lead to the same phase factor b) Two spin configurations related by an inversion of the y-axis. Their topological action differs by a factor of -1.

of a hemisphere of S^3.

As we are only interested in the geometrical phase, we can take a closer look at the topological part of the O(4) NLSM, that is the θ-term:

$$S_{top} = \int d^2x d\tau \frac{i\pi}{\Omega_3} \epsilon_{abcd} n^a \partial_\tau n^b \partial_x n^c \partial_y n^d. \tag{56}$$

Clearly, $\theta = \pi$, which means that a full covering of S^3 with surface area Ω_3 will result in an overall phase of $e^{i\pi} = -1$, whereas a half covering of S^3 leads to a phase factor of $\pm i$. This information will turn out to be crucial when we try to develop an expression for the commutation relation between two spin flips.

4.4 Commutation relations for neighboring spin flips

As mentioned before, we can implement a spin flip in the path integral formalism by interpolating between the two imaginary time-slices before and after the spin-flip. It is now straightforward to calculate the commutation relations for spin flips on nearest neighbor sites as one simply has to compare the phases which are generated by the θ-term (Eq. 56) for both orderings of the flips. This is particularly easy because all configurations in spacetime can be fragmented into unit-cells, which are given by the prisms defined above. The possible processes along with the associated phase factors are listed in Tab. 2 at the end of this chapter.

Two issues arise when we try to dissect the overall configuration into prisms. First of all, we have only defined rules for processes on which the spin on site r on the front left is flipped. Secondly, so far we have only talked about prisms with triangles pointing upwards. The configuration on the diamond that is relevant for the commutator, however, also contains prisms with triangles that point downwards.

The first issue can be resolved very easily by noting that the prism - along with the orientation on its edges - is symmetric under 120 degree rotations in the x-y-plane. Therefore the integration of a prism on which the spin on site r' on the front right is

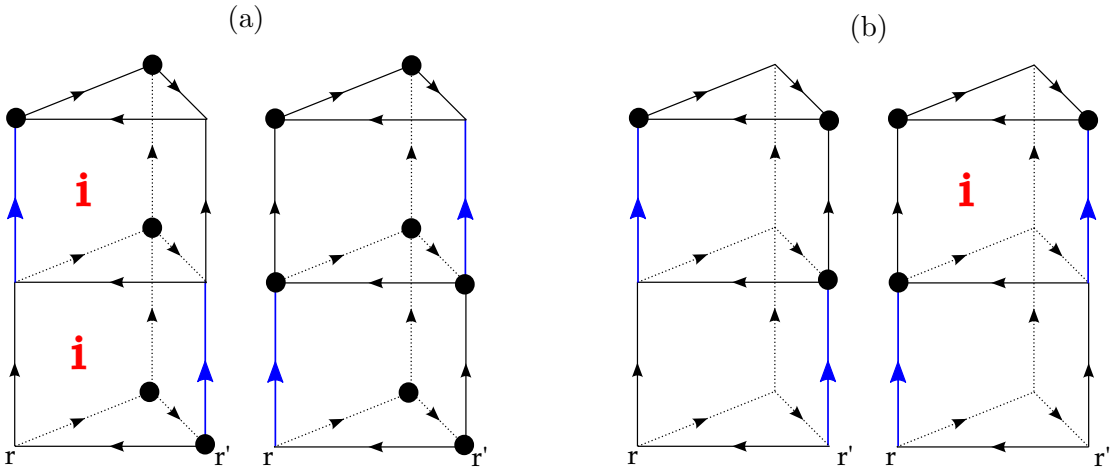

Figure 11: a) Graphical representation of the identity $\tau^x_r \tau^x_{r'} \beta = \tau^x_{r'} \tau^x_r$. The two columns correspond to the two different orders in which both spin-flip operators act. The spin flip process is depicted by an oriented blue edge. As always, sites with a black dot are occupied by a down-spin, whereas sites without a dot are occupied by an up-spin. The two prisms on the left lead to a phase difference of $\beta = (-i) \cdot (-i) = -1$. b) Another spin configuration for which $\beta = i$

flipped, can easily be related to our 'standard' prism by a coordinate transformation (Fig. 10a). In fact, the topological phase for both processes (the original and the rotated one) are exactly the same, as the handedness of the coordinate system and therefore the orientation of the integral is preserved.

We can resolve the second issue by noting that prisms with triangles pointing downwards are related to those with triangles pointing upwards by an inversion of the y-axis (Fig. 10b). This symmetry, however, does not preserve the handedness of the coordinate system and therefore the topological action is related to the original one by a minus sign. This means that if two configurations are partners connected by an inversion symmetry, their geometrical phases are related by complex conjugation. The same conclusion can be obtained by looking at the coordinate-representation of the θ-term (Eq. 56). Clearly $f(x, y, \tau) = \epsilon_{abcd} n^a \partial_\tau n^b \partial_x n^c \partial_y n^d$ is odd under inversion of y if $\vec{n}(x, -y, \tau) = \vec{n}(x, y, \tau)$. Therefore,

$$\int_0^{y'} dy f(x, y, \tau) = -\int_0^{y'} dy f(x, -y, \tau) = -\int_0^{-y'} d(-y) f(x, y, \tau) =$$
$$= \int_0^{-y'} dy f(x, y, \tau) = -\int_{-y'}^{0} dy f(x, y, \tau)$$

Another observation that simplifies the calculation of the commutator is the fact that the θ-term is invariant under $\vec{n} \to -\vec{n}$. Therefore spin configurations that are related by this transformation give the same geometrical phase.

As an example we derive the phase difference for the spin configuration shown in Fig. 11a. All the other configurations are listed in Appendix 3. We will denote the spin-flip

process on site r by the expression τ_r^x and define the phase β by $\tau_r^x \tau_{r'}^x \beta = \tau_{r'}^x \tau_r^x$. The expression τ_r^x should not be interpreted as an operator but merely as a symbol describing the continuous spin flip, the implementation of which is described above.

The first column of each picture corresponds to the order $\tau_r^x \tau_{r'}^x$. We start by looking at the lower prism of the first column: as Tab. 2 only applies to configurations where the spin on the front left is flipped, we have to rotate the prism by 240 degrees. After this transformation the prism describes a process $(\downarrow, \uparrow, \downarrow) \to (\uparrow, \uparrow, \downarrow)$. In our notation, the spins inside the brackets start in the front on the left and then move clockwise, following the orientation of the edges. The phase factor associated with this process is given by Tab. 2 and equal to i.

The second prism is already oriented the right away and we can identify the process $(\uparrow, \downarrow, \uparrow) \to (\downarrow, \downarrow, \uparrow)$ with the phase factor of i. Both of the prisms in the second column of Fig. 11a, which corresponds to the order $\tau_{r'}^x \tau_r^x$, lead to a phase factor of 1 (which is not depicted in the figure).

By comparing both columns we can conclude that for an initial spin configuration $(\uparrow, \downarrow, \uparrow)$, $\beta = -1$. Similar reasoning leads to $\beta = i$ for the initial spin configuration $(\uparrow, \uparrow, \uparrow)$, shown in Fig. 11b.

So far we have not mentioned the contribution to β by triangles on which only one spin is flipped. Indeed, it turns out that every plaquette in the two intertwining hexagons shown in Fig. 8a contributes to the topological action for spin-flip processes. However, as the triangles in question only contain either r or r' they have no information whatsoever about the order in which the spin-flips act. Therefore, as long as we are only interested in the phase difference β, the contributions of triangles outside of the diamond cancel out. We point out that the same conclusion, namely that the commutation relations for spin-flips on neighboring sites r and r' only depend on the configuration on the diamond with vertices r,r',A and B (Fig. 8a) has been drawn for the Chen-Gu model. However, in the case of the NLSM, this is merely an effect caused by our choice of interpolation rules, as adjacent prisms in our construction do not influence one another.

We can summarize the results of Tab. 3 by writing down the following rules for initial spin configurations and their respective β:

1. $(s, s, s) : i$
2. $(s, \bar{s}, s) : i$
3. $(s, s, \bar{s})$: 1
4. $(s, \bar{s}, \bar{s})$: -1

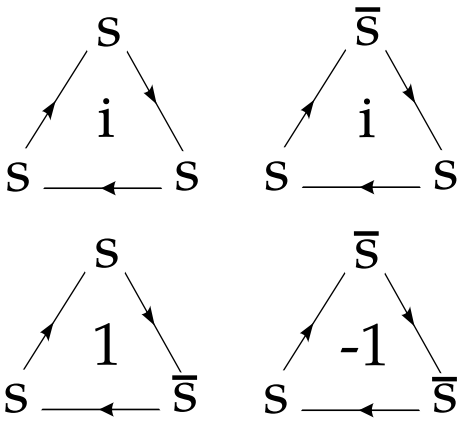

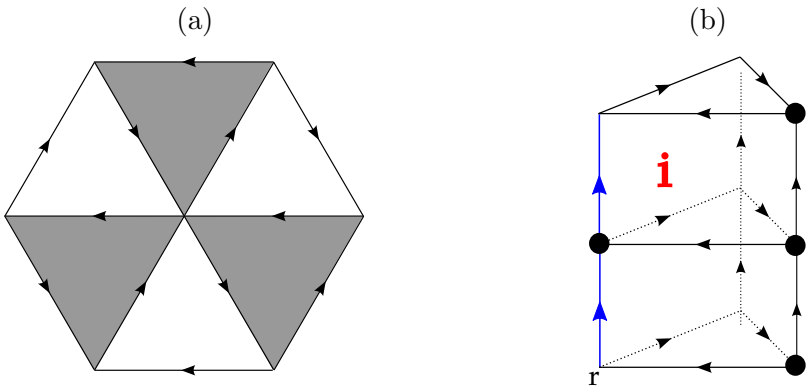

Figure 12: a) The two different classes of triangles. Triangles with the same shading can be related to one another by rotation. b) Spin configuration for the process $(\tau_r^x)^2$.

The β's for triangles pointing downwards can be obtained by complex conjugation. Therefore, if the spins on sites r and r', i.e. the ones that are flipped, point in the same direction, rule 1 and 2 make sure that the overall β is always one. It turns out that the only configurations that lead to an non-trivial overall β of -1 are combinations of rule 3 and 4. These again are exactly the configurations depicted in Fig. 8b. We have therefore shown that in terms of the commutation relations for two neighboring spin-flips, the Chen-Gu construction and the O(4) NLSM coincide.

4.5 Square of the spin flip

Having compared the commutation relations for spin-flips in both models we can now take a closer look at the square of the spin-flip operator, which in the case of the NSLM corresponds to implementing a spin flip twice on the same site. We have already concluded that the eigenvalue of $(\sigma_r^x)^2$ is equal to $\chi(h)$, which only depends on the configuration on the hexagon encircling the site r (Eq. 52).

To make a similar statement about the NLSM, we again implement spin-flips in a continuous way and analyze the geometrical phase that is produced by the θ-term in the action. These phases can easily be obtained by dividing the spin configuration into prisms and applying the rules listed in Table 2. One example for this derivation is given by Fig. 12b. The first prism can be identified with the first line and second column of Tab. 2 and gives a phase factor of 1 whereas the second prism, which corresponds to the second spin-flip on the same site, corresponds to the time reversed version ($\vec{n} \to -\vec{n}$) of the second line and second column of Tab. 2. This process results in a phase factor of i. To find a general rule, it is helpful to note that the phase factor cannot depend on the direction of the spin that is flipped. This follows from the fact that, as each prism is independent from all other prisms, their order in the time-direction does not matter (as long as the ordering is consistent with the underlying processes).

Considering all possible spin configurations one obtains the following rules for triangles

pointing upwards:

1. $(x, s, s) : 1$
2. $(x, \bar{s}, s) : i$

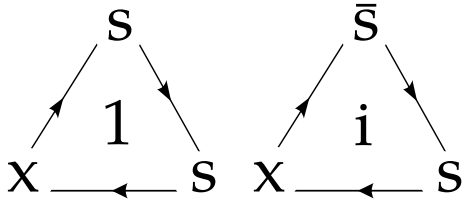

x: arbitary spin direction

Note that the same rules for symmetry transformations as in the sections above apply. These symmetries are given by an inversion of the y-axis and rotations by a multiple of 120 degrees. The hexagon that is relevant for the overall phase associated with $(\tau_r^x)^2$ can be divided into two classes of triangles, which are related by an inversion of the y-axis (Fig. 12a). The elements of each class can be transformed into each other by a rotation Note that two elements of different classes cannot be related to one another by rotation due to the orientation of their edges.

To find an expression for $(\tau_r^x)^2$ acting on a general spin configuration on the hexagon h around r we consider chains of down-spins on h, treating isolated down-spins as a chain with length $l = 0$. Two examples are given in Fig. 7c. There, two configurations are depicted, one of which contains two chains of length $l = 1$ and the other one contains one chain of length $l = 2$. It is clear that at each end of a chain, there is a triangle with spin configuration $(x, \bar{s}, s)$. One might therefore assume that each chain leads to a phase factor of -1. However, this is not true as one has to distinguish between the two classes of triangles. If the chain ends on a triangle that is pointing upwards, the phase factor associated with this triangle is i, for triangles pointing downwards the phase factor is $-i$. Therefore, chains with an even length lead to a phase factor of 1, whereas chains with an odd length lead to a phase factor of -1. This, however, implies the the statement that $(\tau_r^x)^2 \cong \chi(h)$, where $\chi(h)$ is given by Eq. 48.

We have therefore proven that both $(\sigma_r^x)^2$ of the Chen-Gu construction and $(\tau_r^x)^2$ in the NLSM have the same eigenvalues (in case of τ_r^x the geometrical phase replaces the notion of an "eigenvalue") given by $\chi(h)$.

5 Conclusion and Outlook

In this work, we have extend the Chen-Gu construction to (3+1) dimensions for T-reversal invariant SPTs. Furthermore, we have shown that spin-flip operators for both models considered in this paper coincide regarding certain properties. These properties include the commutation relations for neighboring spin-flips and the eigenvalues of two successive identical spin-flips. Being defined on a lattice, the SPT state in the Chen-Gu formalism was already equipped with a natural definition of a spin-flip operator. We have proven that the phase factors arising in the Chen-Gu model for the spin-flip processes listed above are encoded in the topological term of the NLSM. A phase factor of -1 for the commutation of two spin-flips, for example, corresponds to a vortex in the spacetime configuration describing the same process in the NLSM.

Note that all properties of the operator $\tilde{\sigma}_i^x$ that differ from a standard Pauli-matrix σ_i^x directly arise from the dynamical phase factor

$$\prod_{\triangle,\triangledown} \nu_4(g_k, g_l, g_m)$$

that occurs in the definition of $U^i(g)$. Therefore, there is a direct connection between this phase factor and the topological phase that arises from the θ-term in the NLSM. We think that our work can contribute to connecting both models by providing an intuitive interpretation for the rather abstract product of cocycles $\nu_4(g_0, ..., g_n)$ that occurs in the definition of $U^i(g)$.

Given that both models use the group cohomology approach to classify the constructed SPT phases, our results strongly suggest that both models indeed realize the same T-reversal SPT phase. For a final proof, it would be desirable to show that both models realize the same states on their surfaces. It is known that the T-reversal SPT phase that lies within the group-cohomology classification can have $\mathbb{Z}_2$ topological order on its surface. This has been proven for the NLSM but a proof for the Chen-Gu construction is still missing. It is important to note that the surface state in question does not correspond to the standard $\mathbb{Z}_2$ topological order as introduced by Kitaev [11]. Just like in the original model, the elementary excitations e and m are bosonic, the composite quasiparticle is fermionic, and all excitations are mutual semions. The definition of SPT phases however requires the surface state of a (3+1) dimensional system to implement the symmetry T in a way that is not possible in purely (2+1) dimensional systems. Indeed, it can be shown that the bosonic excitations of the $\mathbb{Z}_2$ surface state transform as Kramer's doublets ($T^2 = -1$) and therefore projectively under the symmetry group [3]. This differs from the original version of $\mathbb{Z}_2$ topological order, where all three excitations transform under a linear representation of T so that $T^2 = 1$.

References

[1] I Affleck, T Kennedy, Eh Lieb, and H Tasaki. Rigorous Results on Valence Bond Ground. *Physical review letters*, 59(7):799–802, 1987.

[2] Alexander Altland and Benjamin D Simons. *Condensed Matter Field Theory*. Cambridge University Press, 2 edition, 2010.

[3] Zhen Bi, Alex Rasmussen, Kevin Slagle, and Cenke Xu. Classification and description of bosonic symmetry protected topological phases with semiclassical nonlinear sigma models. *Physical Review B*, 91(13):13, 2015.

[4] F. J. Burnell, Xie Chen, Lukasz Fidkowski, and Ashvin Vishwanath. Exactly soluble model of a 3D symmetry protected topological phase of bosons with surface topological order. *arXiv:1302.7072*, page 9, 2013.

[5] Xie Chen, Fiona J Burnell, Ashvin Vishwanath, and Lukasz Fidkowski. Anomalous Symmetry Fractionalization and Surface Topological Order. *arXiv:1403.6491*, page 12, 2014.

[6] Xie Chen, Zheng Cheng Gu, Zheng Xin Liu, and Xiao Gang Wen. Symmetry protected topological orders and the group cohomology of their symmetry group. *Physical Review B - Condensed Matter and Materials Physics*, 87(15):155114, April 2013.

[7] Andrew M. Essin and Michael Hermele. Classifying fractionalization: Symmetry classification of gapped Z 2 spin liquids in two dimensions. *Physical Review B - Condensed Matter and Materials Physics*, 87(10):1–26, 2013.

[8] Lukasz Fidkowski and Alexei Kitaev. Topological phases of fermions in one dimension. *Physical Review B - Condensed Matter and Materials Physics*, 83(7):075103, February 2011.

[9] E Fradkin. *Field theories of condensed matter physics*. Cambridge University Press, 2 edition, 2013.

[10] M. Z. Hasan and C. L. Kane. Colloquium: Topological insulators. *Reviews of Modern Physics*, 82(4):3045–3067, 2010.

[11] Alexei Kitaev. Fault-tolerant quantum computation by anyons. *Annals of Physics*, 303(1):2–30, July 2003.

[12] Alexei Kitaev. Anyons in an exactly solved model and beyond. *Annals of Physics*, 321(1):2–111, January 2006.

[13] Alexei Kitaev and John Preskill. Topological entanglement entropy. *Physical Review Letters*, 96(11):2–5, 2006.

[14] Lev D. Landau and E.M. Lifschitz. *Statistical Physics-Course of Theoretical Physics*. Pergamon, London, 5 edition, 1958.

[15] R. B. Laughlin. Anomalous quantum Hall effect: An incompressible quantum fluid with fractionally charged excitations. *Physical Review Letters*, 50(18):1395–1398, 1983.

[16] Mikio Nakahara. *Geometry, Topology and Physics*. Institute of Physics Publishing, 2 edition, 2003.

[17] Andreas P. Schnyder, Shinsei Ryu, Akira Furusaki, and Andreas W W Ludwig. Classification of topological insulators and superconductors. *AIP Conference Proceedings*, 1134:10–21, 2009.

[18] Horst Stormer. Nobel Lecture: The fractional quantum Hall effect. *Reviews of Modern Physics*, 71(4):875–889, 1999.

[19] Ari M. Turner, Frank Pollmann, and Erez Berg. Topological phases of one-dimensional fermions: An entanglement point of view. *Physical Review B - Condensed Matter and Materials Physics*, 83(7):1–11, 2011.

[20] Ashvin Vishwanath and T. Senthil. Physics of three-dimensional bosonic topological insulators: Surface-deconfined criticality and quantized magnetoelectric effect. *Physical Review X*, 3(1):25, September 2013.

[21] Kevin Walker and Zhenghan Wang. (3+1)-Tqfts and Topological Insulators. *Frontiers of Physics*, 7(2):150–159, 2012.

[22] Edward Witten. Non-abelian bosonization in two dimensions. *Communications in Mathematical Physics*, 92(4):455–472, 1984.

[23] Cenke Xu and T. Senthil. Wave functions of bosonic symmetry protected topological phases. *Physical Review B - Condensed Matter and Materials Physics*, 87(17):1–10, 2013.

Appendices

A Group cohomology

Let M be an abelian group. Let G be another, not necessarily Abelian, group. If G acts on M as

$$g \cdot (m_1 + m_2) = g \cdot m_1 + g \cdot m_2, \quad g \in G, \quad m_1, m_2 \in M, \tag{57}$$

where $\cdot : G \times M \to M$ should be interpreted as an operator that is yet to be defined, then M can be considered a module on G, or G-module [1]. For our purposes, it is enough to identify M with the Abelian group U(1). Its group elements m_1 and m_2 are then simply phase factors, and the operator $+ : M \times M \to M$ the standard multiplication. If G only contains unitary elements, its action on M is trivial: $g \cdot m_1 = m_1$. If, however G also contains the antiunitary time-reversal operation T, we can define a non-trivial action of G on M by $g \cdot m_1 = m_1^{s(g)}$ where $s(g) = -1$ if $g = T$, and $s(g) = 1$ otherwise. As the elements of M are just phases, this simply means that the group element T leads to a complex conjugation of the module element on which it acts. Following the notation of Chen et al., we denote this 'special' module by $U_T(1)$.

Let $\omega_n : G^n \to M$ and $\mathcal{C}^n(G, M) = \{\omega_n\}$ be the space of all ω_n. For reasons that will become clear later, we will refer to the elements of $\mathcal{C}^n$ as the n-cochains. As the module M is an Abelian group, so is $\mathcal{C}^n(G, M)$ under the chochain multiplication $\omega_n''(g_1, ..., g_n) = \omega_n'(g_1, ..., g_n)\omega_n(g_1, ..., g_n)$. We can introduce a map $d_n : \mathcal{C}^n(G, U_T(1)) \to \mathcal{C}^{n+1}(G, U_T(1))$ defined by

$$\begin{aligned}(d_n\omega_n)(g_1, ..., g_{n+1}) =& (g_1 \cdot \omega_n(g_2, ..., g_{n+1}))\omega_n^{(-1)^{n+1}}(g_1, ..., g_n) \\ &\times \prod_{i=1}^{n} w_n^{(-1)^i}(g_1, ..., g_{i-1}, g_i g_{i+1}, g_{i+2}, ..., g_{n+1}).\end{aligned} \tag{58}$$

Let us now introduce two groups, the group of coboundaries

$$\mathcal{B}^n(G, M) = \{b_n | \omega_n = d_{n-1}\omega_{n-1} | \omega_{n-1} \in \mathcal{C}^{n-1}(G, M)\} \tag{59}$$

and the group of cocycles,

$$\mathcal{Z}^n(G, M) = \{z_n | d_n\omega_n = 1 | \omega_n \in \mathcal{C}^n(G, M)\}. \tag{60}$$

Introducing the equivalence relation $z_n \sim z_n'$ if $z_n' = z_n b_n$ leads to the cohomology group

$$\mathcal{H}(G, M) = \mathcal{Z}^n(G, M)/\sim \tag{61}$$

the elements of which are the respective equivalence classes.

Using another approach to define the cohomology group leads to a clearer interpre-

[1] In fact, G and M have to fulfill other properties that are not important for our purposes.

tation in terms of the less abstract de Rham cohomology of differential forms. We can start by defining functions $\nu_n : G^{n+1} \to M$ that satisfy the equality

$$\begin{aligned} g \cdot \nu(g_0, g_1, ..., g_n) &= \nu^{s(g)}(g_0, g_1, ..., g_n) \\ &= \nu(gg_0, gg_1, ..., gg_n), \quad \forall g \in G \end{aligned} \tag{62}$$

Again the group of n-cochains is given by $\mathcal{C}^n(G, M) = \{\nu_n\}$. There is a one to one correspondence between ν_n and ω_n, given by

$$\omega_n(g_1, ..., g_n) = \nu_n(1, g_1, g_1g_2, ..., g_1...g_n) \equiv \nu_n(1, \tilde{g}_1, \tilde{g}_2, ..., \tilde{g}_n). \tag{63}$$

The map d_n has now the simpler form

$$(d_n\nu_n)(g_0, g_1, ..., g_{n+1}) = \prod_{i=0}^{n+1} \nu_n^{(-1)^i}(g_0, ...g_{i-1}, \hat{g}_i, g_{i+1}, ..., g_{n+1}). \tag{64}$$

where the element with a hat is omitted.

It is easy to prove that $(d_{n+1}d_n\nu_n) = 1$:

$$\begin{aligned} &(d_{n+1}d_n\nu_n)(g_0, g_1, ..., g_n + 2) = \prod_{i=0}^{n+2} (d_n\nu_n)^{(-1)^i}(g_0, ..., \hat{g}_i, ..., g_{n+2}) \\ &= \prod_{i=0}^{n+2} \prod_{j<i} \nu_n^{(-1)^{i+j}}(g_0, ..., \hat{g}_j, ..., \hat{g}_i, ..., g_{n+2}) \prod_{j>i} \nu_n^{(-1)^{i+j-1}}(g_0, ..., \hat{g}_i, ..., \hat{g}_j, ..., g_{n+2}) \\ &= \prod_{i=0}^{n+2} \prod_{j<i} \frac{\nu_n^{(-1)^{i+j}}(g_0, ..., \hat{g}_j, ..., \hat{g}_i, ..., g_{n+2})}{\nu_n^{(-1)^{i+j}}(g_0, ..., \hat{g}_j, ..., \hat{g}_i, ..., g_{n+2})} = 1. \end{aligned}$$

This suggests an interpretation of d_n as some kind of exterior derivative, and indeed as we will show below, this interpretation is justified. The definition of coboundaries and cocycles given by Eq. 59 and Eq. 60 can also be adopted for ν_n and we can write down the cocylce conditions

$$(d_1\nu_1)(g_0, g_1, g_2) = \nu_1(g_1, g_2)\nu_1(g_0, g_1)/\nu_1(g_0, g_2) \tag{65}$$

for n=1 and

$$(d_2\nu_2)(g_0, g_1, g_2, g_3) = \frac{\nu_2(g_1, g_2, g_3)\nu_2(g_0, g_1, g_3)}{\nu_2(g_0, g_2, g_3)\nu_2(g_0, g_1, g_2)} \tag{66}$$

for n = 2. 2-coboundaries fulfill the relation

$$v_2(g_0, g_1, g_2) = \nu_1(g_1, g_2)\nu_1(g_0, g_1)/\nu_1(g_0, g_2). \tag{67}$$

Imagine the elements $(g_0, g_1, ..., g_n)$ lying on a n-dimensional complex with oriented

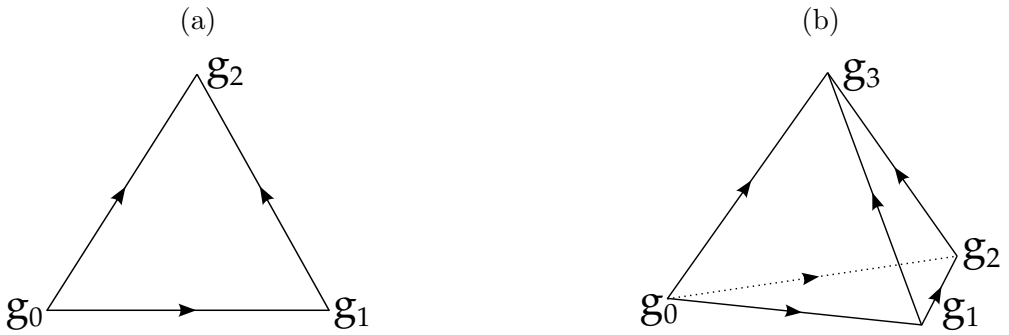

Figure 13: a) Branching structure on a 2 dimensional simplex. b) 3 dimensional simplex.

boundary and let $d\Omega_{n-1}$ be a volume form on this complex. If, for example n = 2, (g_0, g_1, g_2) lie on a triangle with oriented edges (Fig. 13a). The orientation of the edges has to be chosen in a way so that there are no loops. This can be easily achieved by letting the edges always point from lower to higher indices (e.g. from g_0 to g_2). Now, according to Stoke's law, the integral over the volume form can be written as

$$\int_{(g_0,g_1,\ldots,g_n)} d\Omega_{n-1} = \int_{\partial(g_0,g_1,\ldots,g_n)} \Omega_{n-1}, \tag{68}$$

or in case of our example by

$$\int_{(g_0,g_1,g_2)} d\Omega_1 = \int_{g_0}^{g_1} \Omega_1 - \int_{g_0}^{g_2} \Omega_1 + \int_{g_1}^{g_2} \Omega_1. \tag{69}$$

Identifying

$$(d_1\nu_1)(g_0, g_1, g_2) = \exp(i \int_{(g_0,g_1,g_2)} d\Omega_1) \tag{70}$$

and

$$\nu_1(g_i, g_j) = \exp(i \int_{g_i}^{g_j} \Omega_1) \tag{71}$$

we see that Eq. 69 implies Eq. 65, and that $(d_{n+1}d_n\nu_n) = 1 \Leftrightarrow d^2\Omega_n = 0$. Furthermore, we have shown that there is indeed a geometrical interpretation for the ν_n defined above in terms of the De Rham cohomology as we can now identify cocycles $d_n\nu_n = 1$ with closed forms $d\Omega_n = 0$ and coboundaries $\nu_n = d_{n-1}\nu_{n-1}$ with exact forms $\Omega_n = d\Omega_{n-1}$ [16].

B Alternative approach to connecting both theories

The definition of the operator $\tilde{\sigma}_r^x$ in Sec. 4.2 might seem a bit forced or artificial, but its existence appears to be necessary to compare the different phase factors that arise in both models. However, there is another more general approach that leads to the same results. Let us define the operator $\hat{\theta}$ by

$$\hat{\theta}\,|\phi\rangle = \prod_{\triangle,\triangledown} \nu_4(g_k, g_l, g_m)\,|\phi\rangle \tag{72}$$

in analogy with the phase factor associated with the symmetry representation $U^i(g)$ defined in Eq. 21. Consider that, instead of modifying the spin-flip operator in the Chen-Gu model, we use the original Pauli-matrix σ_r^x. To make up for this step backwards, we 'measure' the topological phase factor given by $\hat{\theta}$ after each performed spin-flip. Instead of identifying the eigenvalues of the operator $(\tilde{\sigma}_r^x)^2$ we can now look at the expression

$$\hat{\theta}\sigma_r^x\hat{\theta}\sigma_r^x\,|r,h\rangle = \lambda(r,h)\,|r,h\rangle \tag{73}$$

where σ_r^x is the standard (not modified) Pauli matrix. It is easy to convince oneself that $\lambda(r,h) = \chi(r,h)$, where $\chi(r,h)$ is defined in Eq. 48. Further, we can, instead of obtaining an expression for $\gamma(r,r',A,B)$, which characterizes the commutation relation for neighboring $\tilde{\sigma}^x$ and which is defined in Eq. 55, determine $\Gamma(r,r',A,B)$, defined by

$$\hat{\theta}\sigma_r^x\hat{\theta}\sigma_{r'}^x\,|r,r',h,h'\rangle = \Gamma(r,r',A,B)\hat{\theta}\sigma_{r'}^x\hat{\theta}\sigma_r^x\,|r,r',h,h'\rangle\,. \tag{74}$$

Again, it is straightforward to prove that indeed $\gamma(r,r',A,B) = \Gamma(r,r',A,B)$. We have therefore derived a different, more general approach for the original problem of how to compare the Chen-Gu construction to the NLSM.

C Tables

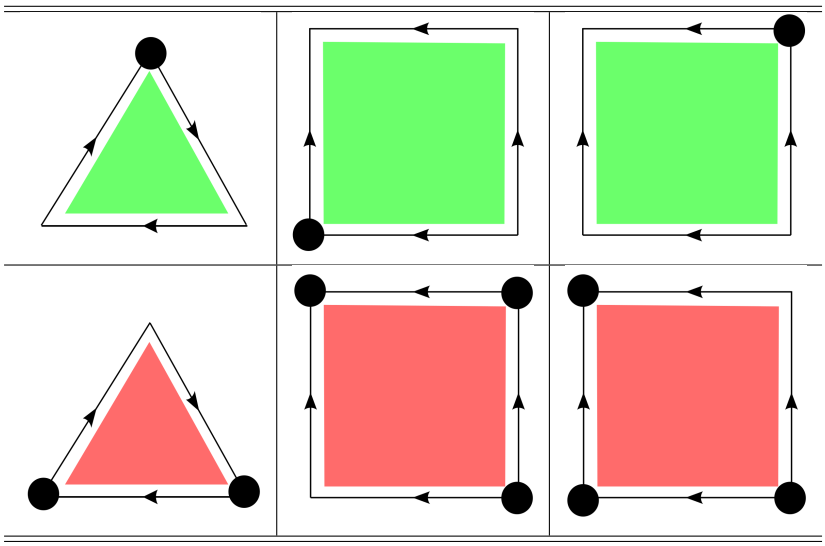

Table 1: Surface configurations that bind a vortex. Green signals an interpolation over the upper hemisphere of S^2, whereas red represents the lower hemisphere of S^2. The lines are related by $\vec{n} \to -\vec{n}$, column two and three are related by a reflection along the diagonal. As always, black dots depict down-spins, empty sites depict up-spins.

ν_2	S_{top}	$\exp(iS_{top})$	ν_2	S_{top}	$\exp(iS_{top})$
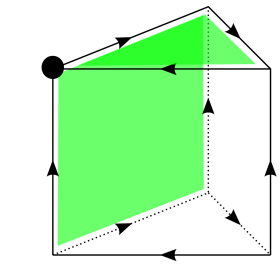			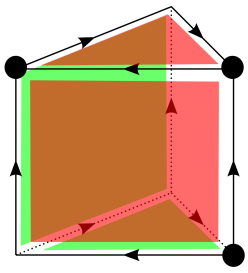		
0	0	1	0	0	1
$(\uparrow,\uparrow,\uparrow) \to (\downarrow,\uparrow,\uparrow)$			$(\uparrow,\uparrow,\downarrow) \to (\downarrow,\uparrow,\downarrow)$		
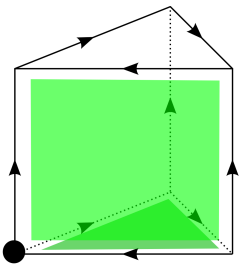			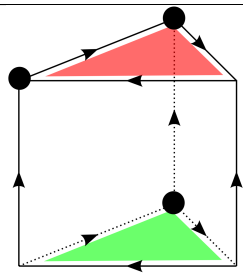		
0	0	1	1	$\frac{\pi}{2}$	i
$(\downarrow,\uparrow,\uparrow) \to (\uparrow,\uparrow,\uparrow)$			$(\uparrow,\downarrow,\uparrow) \to (\downarrow,\downarrow,\uparrow)$		

Table 2: Geometrical phase associated with configurations on a prism. The listed configurations correspond to processes on which the spin on the front right site is flipped. Configurations that are related to the listed ones by either $\vec{n} \to -\vec{n}$ or rotations in the x-y-plane lead to the same phase. The phase factors for prisms with inverted y-axis can be obtained by complex conjugation.

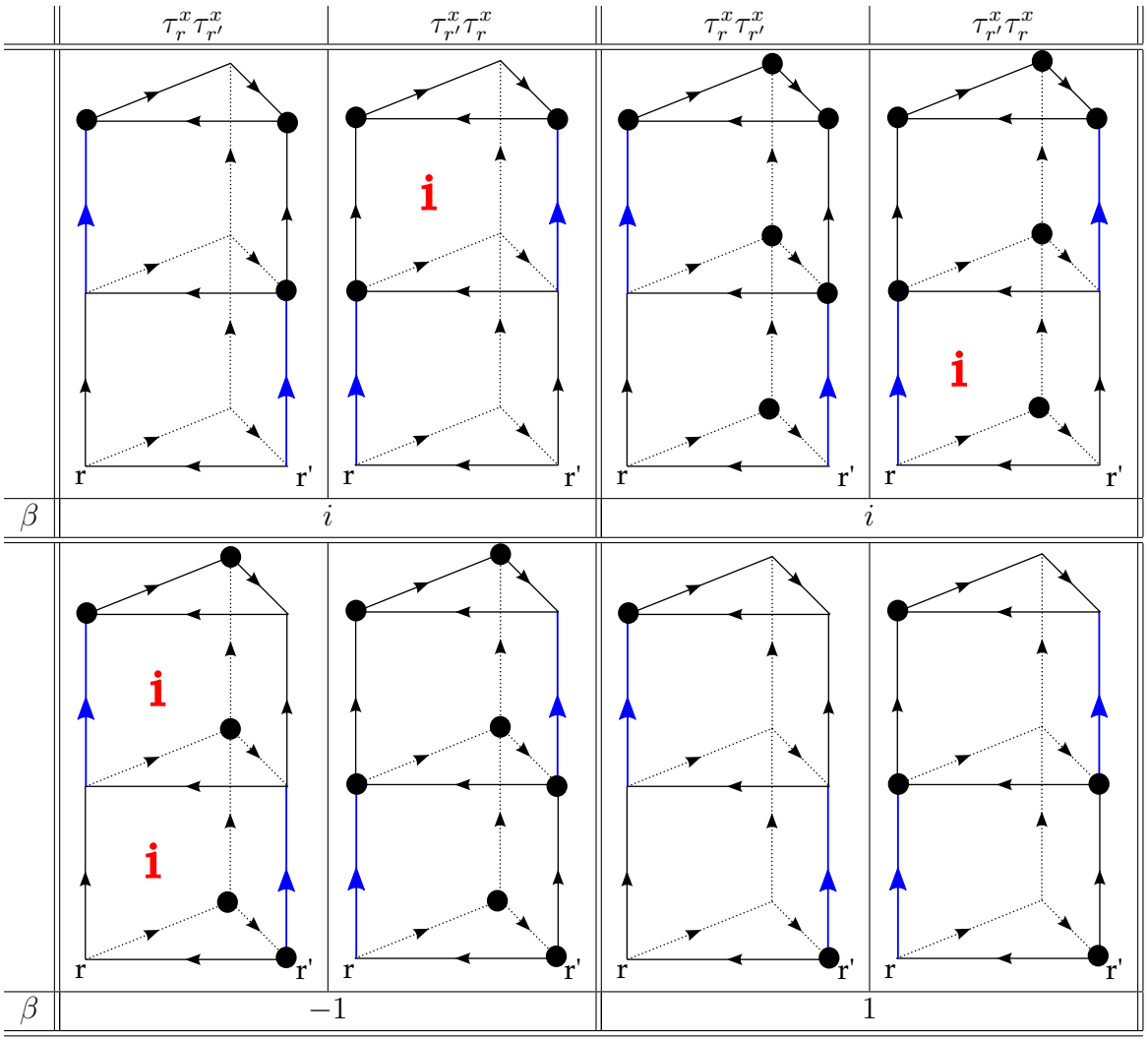

Table 3: Derivation of the phase factor β which is defined by the equality $\tau_r^x\tau_{r'}^x\beta = \tau_{r'}^x\tau_r^x$. All other configurations can either be obtained by $\vec{n} \to -\vec{n}$, which leaves the associated β invariant, or $y \to -y$, which leads to $\beta \to \beta^*$.